Regional water resources availability and vulnerability

Faculty of Natural Sciences and Engineering
University of Ljubljana
(FB5)

Ljubljana, 2016

Lead Author/s	Barbara Čenčur Curk, Petra Žvab Rožič
Lead Authors Coordinator	Barbara Čenčur Curk
Contributor/s	LB, FB5, FB6, FB8, FB10, FB11, FB12, FB14, FB16
Date last release	30. 11. 2016
State of document	Final

Let's grow up together

DRINK ADRIA

Adriatic IPA
Cross Border Cooperation 2007-2013

DRINK ADRIA

Contributors, name and surname	Institution
ITALY	
Ricardo Silvoni Franco Cucchi, Chiara Calligaris	LB - Area Council for Eastern Integrated Water Service of Trieste (CATO), Italy Subcontractor: University of Trieste
SLOVENIA	
Barbara Čenčur Curk, Petra Žvab Rožič, Margarit Nistor, Petra Vrhovnik, Timotej Verbovšek	F5 - University of Ljubljana
CROATIA	
Bruno Kostelić, Dunja Babić	FB6 - Region of Istria
Barbara Karleuša, Ivana Radman	FB8 - Faculty of Civil Engineering, University of Rijeka
SERBIA	
Branislava Matić, Dejan Dimkić, Vladimir Lukić	FB10 - Jaroslav Černi Institute for Water resources Development
ALBANIA	
Arlinda Ibrahimllari, Anisa Aliaj	FB11 - Water Supply and Sewerage Association of Albania (SHUKALB)
BOSNIA AND HERZEGOVINA	
Ninjel Lukovac, Melina Džajić-Valjevac	FB12 - Hydro-Engineering Institute of Sarajevo Faculty of Civil Engineering
MONTENEGRO	
Darko Kovač	FB14 - Public Utility "Vodovod i kanalizacija" Niksic
GREECE	
Vasilis Kanakoudis, Stavroula Tsitsifli	FB16 - Civil Engineering Department, University of Thessaly, Greece

DRINK ADRIA

project partners and can under no circumstances be regarded as reflecting the position of the IPA Adriatic Cross-Border Cooperation Programme Authorities".

Table of Contents

DRINK ADRIA

1. INTRODUCTION

One of the objectives was to assess present and future vulnerability of water resources based on a jointly elaborated methodology. The work has been focused on the identification of drivers influencing vulnerability, the evaluation of the vulnerability of water resouces as well as the assessment and classification of drinking water risks under climate change. The common methodology has been adopted and capitalised from the CC-WARE project, funded within South-east Europe Programme. Methodology is presented in final CC-WARE WP3 report (CC-WARE, 2014a). Within the DRINKADRIA project this methodology was used to asses the vulnerability of water resources in the IPA Adriatic territory that is presented in this report. Description of the methodology is summarized from the report of the CC-WARE project (CC-WARE 2014a), while the results show the state of the area (countries) included in the IPA Adriatic programme. For water quality only the present vulnerability was calculated and consequantly also the integrated assesment of water resources availability to climate change only for present was presented.

The applied methodology of vulnerability assessment was performed on regional scale with large spatial resolution (25 x 25 km) and generalization of data, therefore diversity of the terrain and climate data in a local scale can not be expressed. Additionaly, there was insufficient detailed data on water demand for all countries. The resulting assessment of the integrated vulnerability on the transnational level gives a generalized representation on the main trends and impacts of the different driving forces and not local situations. The latter were elaborated for pilot areas within activities 4.1 (climate downscaling), 4.2 (water availability and WEI) and 4.3 (water quality).

The acquired knowledge indicates the need for higher degree of harmonisation of input data on national level, as well as development of future investigations in terms of smaller spatial discretization, further development of the applied methodology and validation of results obtained on the basis of climatological input data with results of hydrological monitoring of surface and ground water runoff and water demand.

DRINK ADRIA

2. VULNERABILITY OF WATER RESOURCES IN THE IPA ADRIATIC AREA

Concern about the potential effects of climate change on water supply and water demand is growing. Water resources vulnerability is a critical issue to be faced by society in the near future. Current variability and future climate change are affecting water supply and demand over all water-using sectors. Consequently, water scarcity is increasing.

Vulnerability of freshwater resources as potential drinking water resources is characterised by several indicators: describing water availability and increasing demand and the future qualitative state of the system compared to drinking water standards.

Land use may significantly influence the quantity of the water resources, water demand and overall water quality. A methodology for determining water resources vulnerability regarding quantity and quality shall take into account also extreme natural events and the multiple impact of the land use. By classifying the water resources vulnerability, critical areas can be identified, where water resources stay under risk. The knowledge of the areal distribution of vulnerable water resources is an important prerequisite for sustainable management of the relevant areas.

The Intergovernmental Panel on Climate Change (IPCC) describes vulnerability as a function of impact and adaptive capacity and 'the degree to which a system (water resources) is susceptible to, or unable to cope with, adverse effects of climate change, including climate variability and extremes' (IPCC, 2003). 'Vulnerability is a function of the character, magnitude and rate of climate variation to which a system is exposed, its sensitivity and its adaptive capacity' (IPCC, 2007). The methodology applied in the CC-WARE project builds on this description of vulnerability by examining the exposure (predicted changes in the climate), sensitivity (the responsiveness of a system to climatic influences) and adaptive capacity (the ability of a system to adjust to climate change) of a range of indicators. Described methodology has been applied to the area IPA area in the DRINKADRIA project.

Exposure, sensitivity, potential impact and adaptive capacity (Figure 1) are all considered in the evaluation of vulnerability to a defined climate change stressor such as temperature increases (Local Government Association of South Australia, 2012).

In CC-WARE project impacts of climate, land use and demographic changes on water resources were analyzed.

DRINK ADRIA
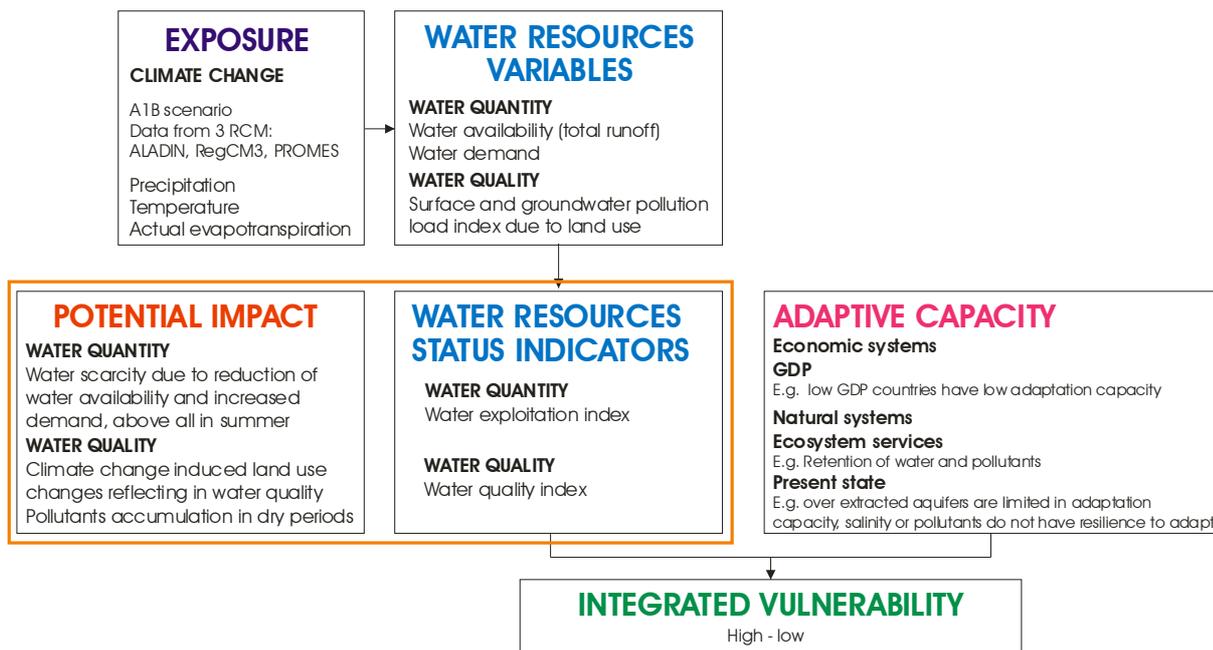
Figure 1: Components of Vulnerability (CC-WARE, 2014a)

Exposure is the change expected in the climate for a range of variables including temperature and precipitation. Sensitivity is the degree to which systems respond to the changes. For example less precipitation may reflect in substantial reduction of water availability in a small river basin or aquifer.

Adaptive capacity describes how well a system can adapt or modify to cope with the climate changes to which it is exposed to reduce harm. Examples of natural systems with low adaptive capacity are those with a limited gene pool and as a result a limited capacity to evolve, over extraction of ground or surface water, salinity or environmental pollutants that do not have the resilience to adapt. Economic systems that have minimal opportunities to increase income would also struggle to adapt to climate changes. Social systems that are disrupted have poor communication networks etc. are also likely to be limited in their capacity to adapt. When the adaptive capacity of a system is reduced, it is considered to be more vulnerable to the impacts of climate change. By considering adaptive capacity it is possible to avoid attending to impacts that may be reduced by the system itself with minimal outside help, or putting systems that have no capacity to adapt as a low priority with the result that more harm occurs than expected. (Local Government Association of South Australia, 2012)

The ecosystem services and GDP were applied as adaptive capacity indicators. When the ecosystem services are high (e.g. the ecosystem is in a sound state and provides a lot of services at low costs) the society saves financial resources while in the opposite case we find a degraded ecosystem where the society needs large investments to replace the ecosystem functions by technical measures.

Integrated water resources vulnerability is an overall indicator characterized by set of indicators referring to water quantity, water quality and adaptive capacity (Figure 1).

From water resource management perspective, vulnerability can be defined as: *the characteristics of water resources system's weakness and flaws that make the system difficult to be functional in the face of socioeconomic and environmental change* (UNEP 2009). Thus, the vulnerability should be measured in terms of:

(i) exposure of a water resources system to stressors at the river basin scale; and

(ii) capacity of the ecosystem and society to cope with the threats to the healthy functionality of a water system (UNEP 2009).

Vulnerability corresponds to changes, which can be compared to a reference situation (e.g. differences between the past/present and future state). However the determination of the changes needs the estimation of the present and the future values of the relevant indicators. Besides, vulnerability cannot be measured, but can be assessed with the help of indicators.

"Overlay/index method" was used for assessment of vulnerability on a national scale (FOOTPRINT 2006). This method is easier to understand than the more complex physical based models and therefore more suitable to use for none-modelers and also more appropriate to enhance the participatory process. To discriminate between different levels of vulnerability (e.g. three classes low/moderate/high), it is necessary to combine all quantities into a single measure.

3. CLIMATE AND CLIMATE CHANGE

The climate is the main natural driver of the variability in the water resources, and atmospheric precipitation, air temperature and evapotranspiration are commonly used for assessing and forecasting the water availability. Generally, the precipitation deficit associated with high temperature and evapotranspiration values define meteorological, agricultural and hydrological drought, while the precipitation amounts exceeding the multiannual averages over an area refill the water resources.

The main objective is to provide climatic indicators relevant for analysing the water resources vulnerability in the IPA Adriatic region. The data will be available for the activities focused on assessing the vulnerability of the water resources.

For climate change data results from the CC-WaterS (CC-WaterS, 2010) project were used. Climate change data were obtained from three RCMs (RegCM3 – ITCP, Aladin – CNRM, Promes – UCLM), based on A1B scenario.

The CC-WaterS data base comprises daily and monthly temperature and precipitation derived from three RCMs, namely RegCM3, ALADIN-Climate and PROMES, extended from 1961 to 2100, at 25-km spatial resolution. RegCM3 is the third generation of the RCM originally developed at the National Center for Atmospheric Research during the late 1980s and early 1990s. The model is driven by the GCM ECHAM5-r3, it uses a dynamical downscaling, and it is nowadays supported by the Abdus Salam International Centre for Theoretical Physics (ICTP) in Trieste, Italy (Elguindi et al., 2007). ALADIN-Climate was developed at Centre National de Recherche Meteorologique (CNRM), and it is downscaled from the ARPEGE-Climate as a driver for the IPCC climate scenarios over the European domain (Spiridonov et al., 2005; Farda et al., 2010). PROMES is a mesoscale atmospheric model developed by MOMAC (MOdelizacion para el Medio Ambiente y el Clima) research group at the Complutense University of Madrid (UCM) and the University of Castilla-La Mancha (UCLM) (Castro et al., 1993; Gaertner et al., 2010), and it is driven by the GCM HADCM3Q0.

The initial simulation results of RegCM3, ALADIN-Climate and PROMES were available from the ENSEMBLES project (Hewitt, 2004), and they were selected because (1) their spatial extent covers the full study area of CC-WaterS, (2) they provided good performance in the simulation of historic climate conditions, and (3) each of them uses a different driving GCM.

A1B Scenario: A1B SRES IPCC scenario, which presumes balanced energy sources within a consistent economic growth, into the context of increasing population until the mid-21st century, and rapid introduction of more efficient technologies (IPCC TAR WG1, 2001).

BIAS Correction: The RCMs outputs were bias corrected using the quantile mapping technique (Déqué, 2007; Formayer and Haas, 2010) based on daily observations extracted from the E-OBS data base v2.0 (CC-WaterS, 2010). E-OBS (Haylock et al., 2008) is an European 25 km-spatial resolution gridded temperature and precipitation data set compiled from daily weather station measurements. Their ability to reproduce the temperature and precipitation was tested both locally (Busuioc et al., 2010) and at European scale (CC-WaterS, 2010). The results showed that differences between both observations and model control runs exist and the results of different RCMs may differ significantly especially in mountainous areas (CC-WaterS, 2010). The quantile mapping technique was used to calibrate each RCM for the control period 1951-2000. The correction method is based on using the differences of the empirical cumulative density functions (CDF) of each model and observation data (E-OBS; Haylock et al., 2008) and it is applied to the

model data such that the statistics of the observations are retained. For the scenario period, the CDFs were calculated for the periods 2001-2025, 2026-2050, 2051-2075 and 2076-2100 and applied in a way, that allows the production of continuous bias corrected time series from 1951-2100 (1951-2050 for PROMES) (CCWaterS, 2010).

The use of the updated E-OBS data sets (v10.0, released in April 2014) in the project CC-WARE improved the bias corrected precipitation in some areas (e.g. Northern Carpathians), while the general pattern remained similar at regional scale.

Ensemble: The outputs of the three models were aggregated for each season by calculating the arithmetic mean for every grid cell.

In CC-WARE and DRINKADRIA project the following time intervals were used:

- 1961-1990 (baseline climate; B);

- 1991-2020 (present climate; P);

- 2021-2050 (future climate; F).

Far future period 2071-2100 was not selected for the DRINKADRIA study due to large uncertainties.

3.1   Determination of climate variables and indicators

Main climate variables are:

- precipitation (RR),
- temperature (T) and
- potential and actual evapotranspiration (PET and AET).

Additional climate variables, which were used for the description of climate, are:

- De Martonne's Index of Aridity

3.1.1   Precipitation (RR) and temperature (T)

Precipitation (RR) and **temperature (T)** data were obtained from the ensemble data set from three RCM models (RegCM3, ALADIN-Climate and PROMES), as described in introduction to this chapter.

3.1.2   Potential evapotranspiration (PET)

The **potential evapotranspiration (PET)** is the maximum possible amount of water resulted from evaporation and transpiration occurring from an area completely and uniformly covered with vegetation, with unlimited water supply without advection and heating (Dingman, 1992; McMahon et al., 2013). The potential evapotranspiration is calculated using the Thornthwaite approach (1974), utilizing solely temperature data of the regional climate models. We used the R-Package SPEI (Beguería and Vicente-Serrano, 2010; Vicente-Serrano et al., 2010) to calculate the PET using the Thornthwaite's formula (Thornthwaite, 1948):

$$PET_m = 16 \left(\frac{L}{12}\right) \left(\frac{N}{30}\right) \left(\frac{10\overline{T}_m}{I}\right)^\alpha \qquad (1)$$

where
PET_m = monthly potential evapotranspiration [mm];
L = average day length of the month being calculated [h];
N = number of days in the month being calculated [-];
$\bar{T}_m$ = average monthly temperature [℃]; $PET_m = 0$ if $\bar{T}_m < 0$
I = heat index:

$$I = \sum_{i=1}^{12} \left(\frac{\bar{T}_{mi}}{5} \right)^{1.514} \tag{1.1}$$

$$\alpha = (6.75 \cdot 10^{-7}) \cdot I^3 - (7.71 \cdot 10^{-5}) \cdot I^2 + (1.791 \cdot 10^{-2}) \cdot I + 0.49239 \tag{1.2}$$

3.1.3 Actual evapotranspiration (AET)

The **actual evapotranspiration (AET)** is a key component for catchment and water balance studies, representing the real evapotranspiration occurring over a certain area in a specific period. The AET was calculated with the Budyko's original equation (Budyko, 1974, Gerrits et al. 2009) according to annual PET and precipitation:

$$\frac{AET_a}{RR_a} = \left[\phi * \tanh\left(\frac{1}{\phi} \right) * (1 - \exp^{-\phi}) \right]^{0.5} \tag{2}$$

where RR_a denotes mean annual rainfall and φ is Budyko Aridity Index:

$$\phi = \frac{PET_a}{RR_a} \tag{2.1}$$

where PET_a is annual potential evapotranspiration.

The Budyko framework is frequently applied to assess actual evapotranspiration on a catchment scale (e.g. Oudin et al., 2008; Roderick et al., 2011; Zhang et al., 2008, 2004, 2001) and has shown satisfactory results. Budyko (1974) considered watersheds with area larger than 1000 km² to minimize the effects of groundwater flows that he assumed to be negligible. Under these conditions he obtained empirically the Budyko curves by plotting the watershed data and fitting with a smooth curve. This is a tool to estimate total runoff from such watersheds. In DRINKADRIA, the spatial scale is 0.25° grid cell, resulting in an area of about 625 km² and it is assumed that Budyko curves can be applied, since the methodology has been applied also to smaller catchments (Oudin et al., 2008; Zhang et al., 2001, 2004, 2008), where validation using observed data show reasonable results. Nevertheless we have to be aware that this is an approximation, since for more precise results Budyko curves have to be modified on the basis of runoff observations, which are not available for the whole IPA Adriatic region. Furthermore long term annual values of rainfall and potential evapotranspiration are used (1991-2020; 2021-2050) as a basis. Therefore the precondition, that the storage term within an area can be neglected, is also considered.

Additional uncertainties of AET results arise because AET is derived from modelled precipitation data, which were bias corrected with E-OBS data base. In spite of that in some regions AET show significant errors, which is especially the case for some mountainous areas. Therefore in these areas results have to be additionally interpreted.

DRINK ADRIA

3.1.4 De Martonne's Index of Aridity

At almost 90 years since its creation, de Martonne Aridity Index (*MA*) still proves its utility for evaluating the water availability in an area (Baltas, 2007; Maliva and Missimer, 2012). The annual value of the index was calculated by the equation (4) (Doerr, 1963), while the corresponding precipitation amounts and climatic classification can be followed in the Table 3 (Baltas, 2007).

$$MA = \frac{RR}{T+10} \tag{3}$$

where RR [mm] is the annual precipitation and T [℃] the annual mean temperature.

Table 1: De Martonne index aridity classification and corresponding precipitation amounts (Baltas, 2007).

Aridity classification	MA	Precipitation (mm)
Dry	< 10.0	< 200.0
Semi-dry	10.0 - 19.9	200.0 - 399.9
Mediterranean	20.0 - 23.9	400.0 - 499.9
Semi-humid	24.0 - 27.9	500.0 - 599.9
Humid	28.0 - 34.9	600.0 - 699.9
Very humid	35.0 - 55.0	700.0 - 800.0
Extremely humid	>55.0	>800.0

3.2 Maps of climate variables in the IPA ADRIATIC region

Climate variables maps were elaborated based on grids and interpolation. Spatial resolution is 0.25°, which is approximately 25 km when projected. All climate variables maps present average value for each grid cell for particular period.

Due to many local coordinate projected systems (e.g. Gauss-Krüger D48 used in Slovenia, another local Gauss-Krueger projected system for Serbia etc.) it was decided to use the most common geographic system WGS1984. Units of this geographic system are latitude and longitude degrees. Consequently, cell size of all raster data was fixed to 0.25° x 0.25° to be consistent with other raster data and snapping of the raster cells was set in ArcGIS Environmental settings. For some layers, data was received or calculated in geographic system ETRS89, using slightly different ellipsoid (GRS80 ellipsoid) than WGS84 system (WGS84 ellipsoid), but the differences in ellipsoid is less than a millimeter in the polar axis, leading to maximum half of the meter in projection, and is as such completely negligible for the purpose of the project data, having cell size of 0.25° x 0.25°.

For estimation of impact of climate change on climate variables, relative changes of absolute values were calculated as:

$$\Delta \mathrm{Var}(F\text{-}P) = \frac{Var\_F - Var\_P}{Var\_P} \tag{4.1}$$

$$\Delta \mathrm{Var}(P\text{-}B) = \frac{Var\_P - Var\_B}{Var\_B} \tag{4.2}$$

where *Var* is climate variable (P, AET, PET) and indexes *F* mean future (2021 – 2050), *P* present (1991 – 2020) and *B* base period (1961-1990).

DRINK ADRIA

3.2.1 Temperature

Differences in the seasonal temperature (^{o}C) according to ensemble of RegCM3, ALADIN and PROMES models between future (2021-2050) and present (1991-2020) period are presented in Figure 2.

(a)

(b)
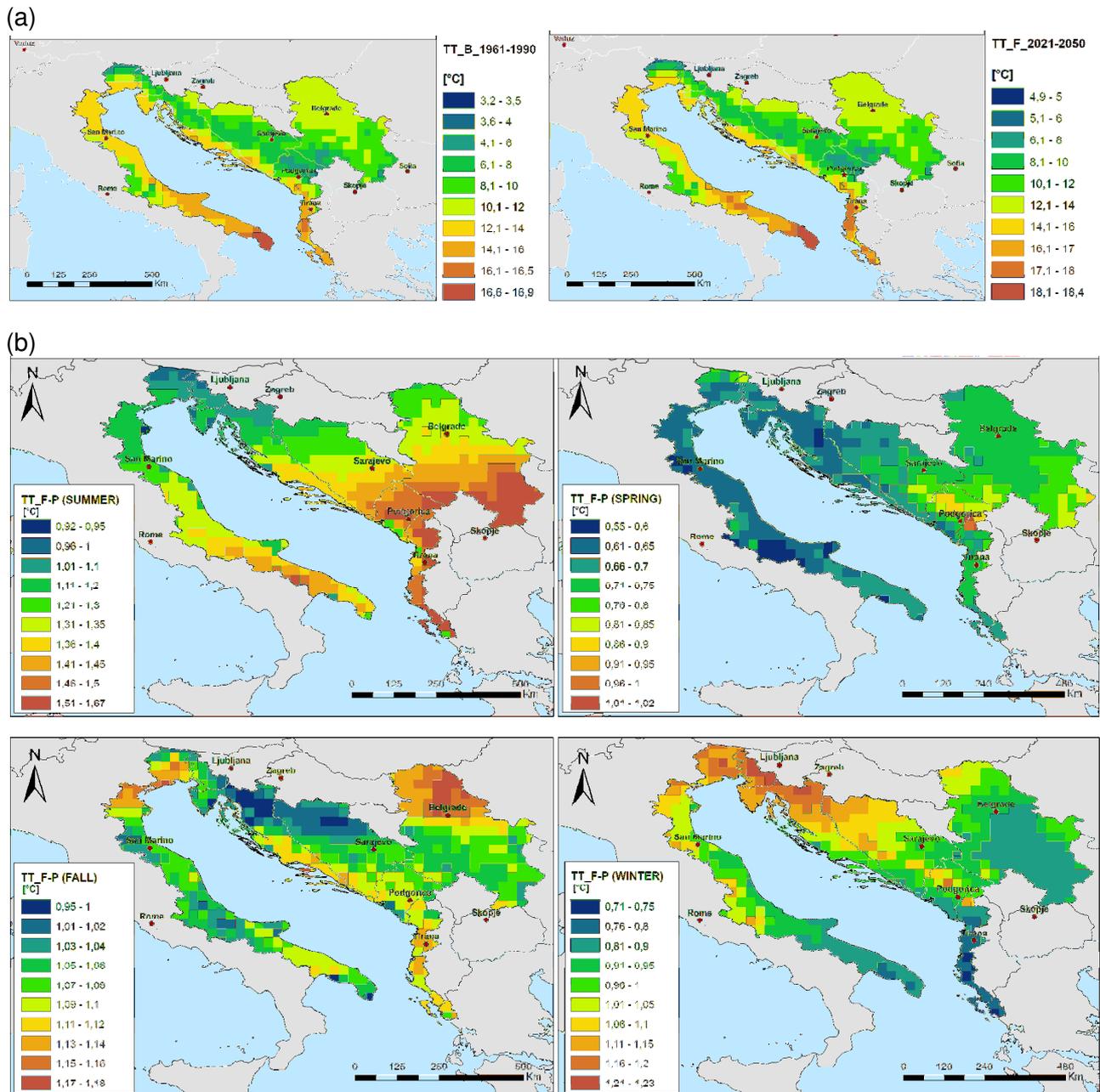
Figure 2 (a) Temperature for baseline (B) and future (F) period based on mean annual ensemble values of RegCM3, ALADIN and PROMES models. (b) Differences in average temperature values (^{o}C) between future (2021-2050) and present (1991-2020) period for fall, winter, spring and summer based on mean ensemble values of RegCM3, ALADIN and PROMES models.

DRINK ADRIA

According to the comparison of future and present mean temperatures found by selected models suggest increase of temperature in individual regions in all seasons. The highest and also most extensive temperature increase occur during the summer in S Serbia, Central and SE Montenegro, E and S Albania, Corfu and partly in SE Italy. The highest temperature increase in spring are in small area of N Albania, in fall in NE Italy, northern part of Serbia and on southern Croatian Islands, while in winter the highest increase occur in Slovenian part of Alps and Dinarides, northern Dinarides in Croatia and E Italy (eastern Po Valley). Generally, the highest changes in temperatures are shown in summer and winter, while in spring the trend of changes are significally lower. Among regions the highest increasing trend is present in central Balkan Peninsula (Serbia, BIH, Montenegro, Albania) in all seasons, with a small difference in winter where the highest increases occur in S Alps and N part of Dinarides, resulting less snow in the future and consequently less water reserves in rivers for spring and summer periods.

Temperature values are for most of the partner countries in adequate range regarding observed data and are acceptable for water balance calculations.

3.2.2 Annual precipitation

The ensemble precipitation for base (1961-1990), present (1991-2020) and future (2021-2050) period according to ensemble of RegCM3, ALADIN and PROMES models are presented in Figure 3. Distribution of precipitation in all periods generally follow the geomorphological characteristics of the area and a decreasing trend is observed in the future. The highest precipitation is observed in Alps, Dinarides and Apenines, but in Dinarides (in BIH) in the future a significant decreasing trend in rainfall is observed. In Central Balkan, S Albania, Corfu and central part of E Italy (E Emiglia Romagna and Marche regions) lower precipitation occur (yellow), while the lowest precipitation is in southern half of E Italy (Abruzzo, Molise and Puglia regions) and the entire eastern half of Serbia, but in Serbia rather increasing precipitation trend is observed in the future.
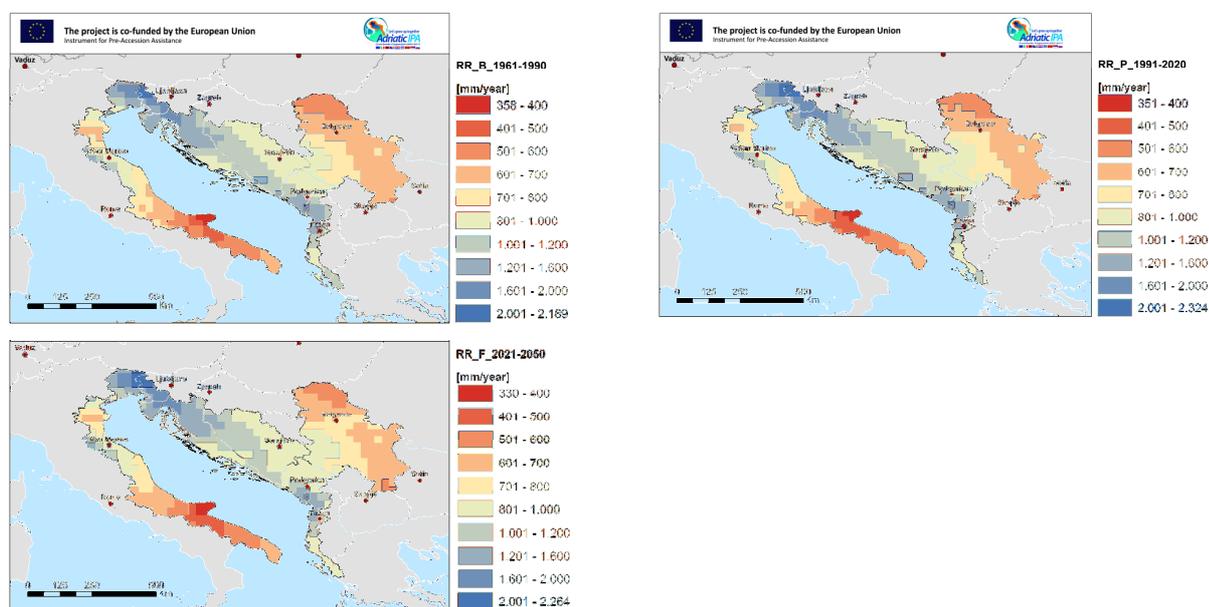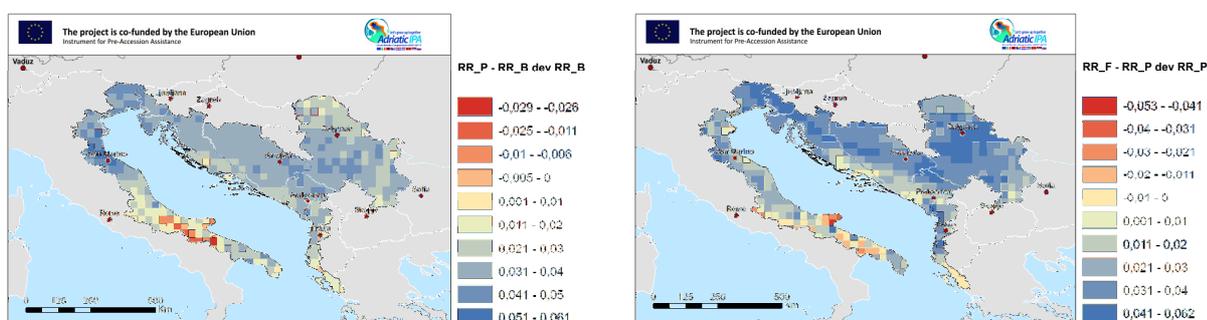

Figure 3: Annual precipitation amount for baseline (B), present (P) and future (F) period based on mean annual ensemble values of RegCM3, ALADIN and PROMES models.

The precipitation maps were compared with measured data for baseline period in partner countries in order to check the plausibility of the results. For most countries the pattern of modelled precipitation is in compliance with measured data. In this point it has to be stressed that this is a regional analysis with the coarse spatial resolution (25 km grid), based on EOBS data base, which has deficiency in underestimated values in mountainous areas, which is the case in the Alps (north-eastern Italy and north-western Slovenia), Apennines (central Italy) and Dinarides (Croatia, BiH, south-west Serbia). Besides, local spatial heterogeneities are however not captured by the coarse spatial resolution. Precipitation is also underestimated in eastern central Serbia and Gargano peninsula in Italy.

Relative differences in precipitation between the present (1991-2020) and base (1961-1990) period and between the future (2021-2050) and present (1991-2020) period are presented in Figure 4. The changes in precipitation show generally positive trends (increasing of precipitation) both for the present in relation to the base as well as for the future in relation to the present. Significal decreasing of precipitation trends are noticeable only in individual parts of the E Italy (Puglia region).

Figure 4: Relative changes in annual precipitation amount between present - base period and future - present period based on mean annual ensemble values of RegCM3, ALADIN and PROMES models.
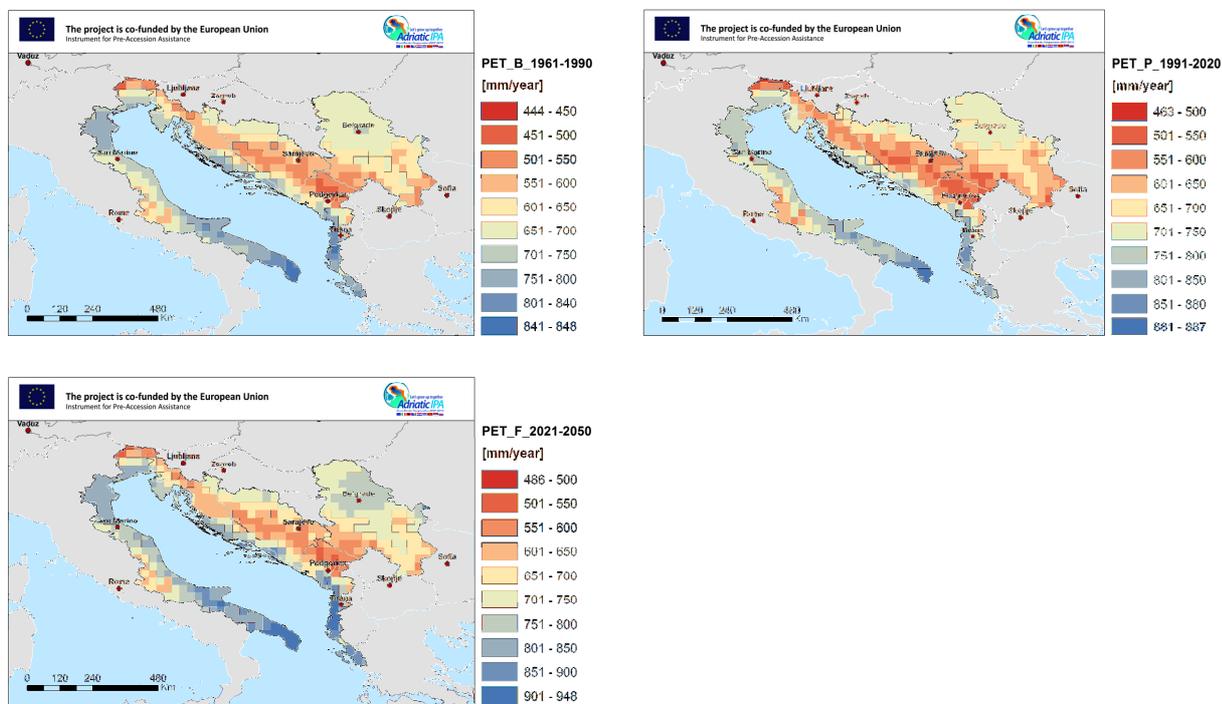
3.2.3 Potential annual evapotranspiration (PET)

Annual potential evapotranspiration (PET) values calculated according to Thornthwaite formula (see eq. 2) on the basis of T derived by the ensemble of RegCM3, ALADIN and PROMES models for baseline, present and future period are presented in Figure 5. According to the equation PET depends on the temperature, which is reflected on the similarity of the pattern of the results obtained. Low PTE are obtained in Alps, Dinarides and Apenines in the areas of low temperatures, while high PTE are along E Italy, W coast of Balkan peninsula (from Central Criatia to Greece) and in future also central Serbia. While the base and future conditions show a similar pattern, in present some significant differences occur. In present period the greater part of eastern Italy (from Po plain to Gargano Promotory) indicates lower PTE as well as N Alps and Dinarides the lowest. Relatively higher PTE in present period regarding to other to periods are in Central Balkan (S BIH, W Serbia and SE Montenegro).

Relative differences in potential evapotranspiration between the present (1991-2020) and base (1961-1990) period and between the future (2021-2050) and present (1991-2020) period are shown in Figure 6. In both cases (present-base, future-present), the relative changes are up to 8%. Calculation between present and base period show the lowest differences in grather part of E Italy and W Balkan Peninsula (mostly coast). Slightly larger differences are in southern part of E Italy,

Po plain, and the rest of Balkan area, while the biggest in Alps, E Serbia and Central Montenegro. The calculations between future and present period show relative slightly bigger changes of PTE in S part od observed area (SE Italy, SW Croatian coast, central Montenegro, the whole Albania, Corfu and S Serbia).

Figure 5: Annual potential evapotranspiration based on mean annual ensemble values of RegCM3, ALADIN and PROMES models for base, present and future period.
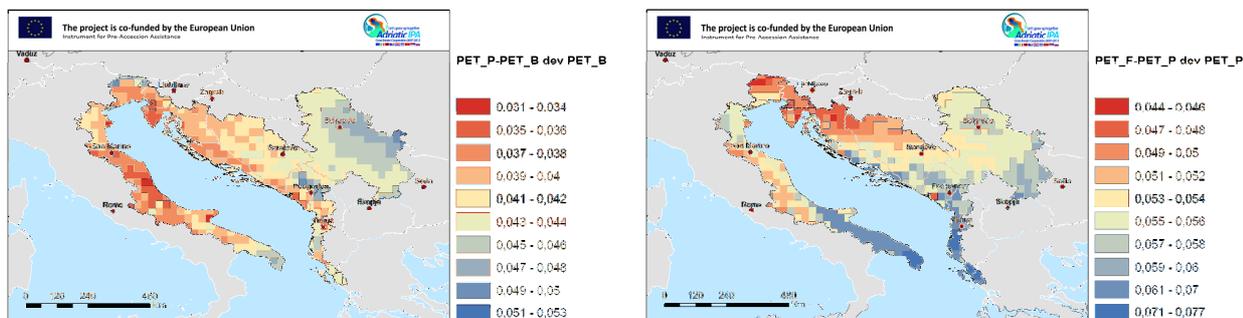
Figure 6: Relative changes of annual potential evapotranspiration between present - base period and future - present period based on mean annual ensemble values of RegCM3, ALADIN and PROMES models.

3.2.4 Annual actual evapotranspiration (AET)

Annual actual evapotranspiration (AET) values calculated on the basis of PET and precipitation estimates derived by the ensemble of RegCM3, ALADIN and PROMES models for baseline, present and future period are presented in Figure 7. High annual AET for all periods is observed in mid-northern and south Italy, in W Slovenia, most part of Croatia, along the whole eastern Adriatic

coast (Croatia, BiH, Montenegro, Albania and Corfu), northern BiH and in the future also in central Serbia. The increasing trend in the future can be observed and is the most significant in BiH and central Serbia. Low AET occur for all periods in mid-eastern Italy (Puglia region – Gargano Promotory), eastrn part of Montenegro and N and S Serbia.

AET maps were compared to calculated/modelled national AET data. AET is calculated indirect with use of PET, which is underestimated in lowland areas, consequently, AET is lower than national modelled AET values in many lowland areas of the study area. In some cases AET is higher (e.g. Alps, Dinarides) than national modelled values. Due to the coarse spatial resolution (25 km grid) local spatial heterogeneities are however not captured, which is the case of north-eastern Italy, where modelled AET on smaller scale are very scattered, but within the range, except for mountainous area.
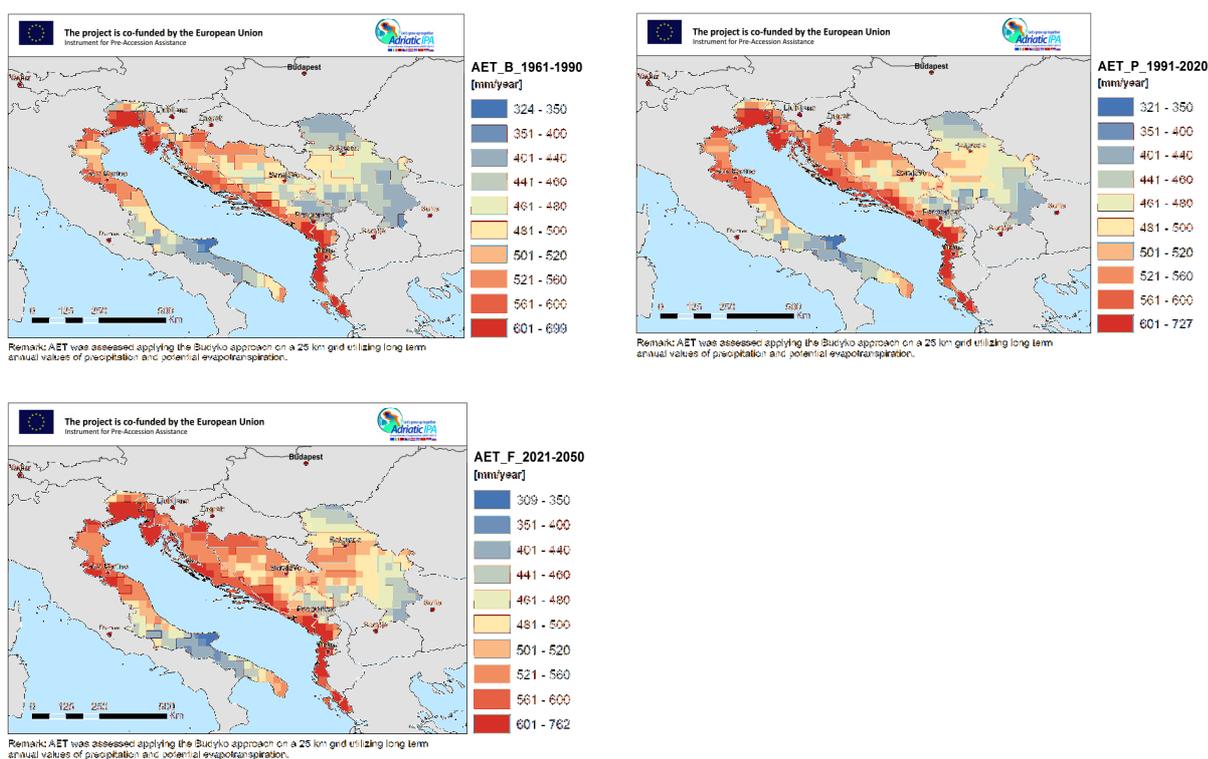
Figure 7: Annual actual evapotranspiration based on mean annual ensemble values of RegCM3, ALADIN and PROMES models for present and future period.

The AET pattern will be preserved in the future, but general increasing in the absolute values are estimated in the future (Figures 7 and 8). Relative differences in precipitation between the present (1991-2020) and base (1961-1990) period (Figure 8) show relative increasing of annual AET in mid-northern Italy (up to 6 %), W Slovenia, northern half of Croatia, most of BiH and Montenegro, central Albania and large part of Serbia without the north and partly south-east. Relative differneces between the future (2021-2050) and present (1991-2020) period (Figure 8) show similar increasing and even more significant pattern of changes. The AET will be even more higher which is especially seen in Serbia and the central part of Balkan Peninsula. The only decrease of AET are observed for both estimated comparison in mid-eastern Italy (Puglia region – Gargano Promotory).
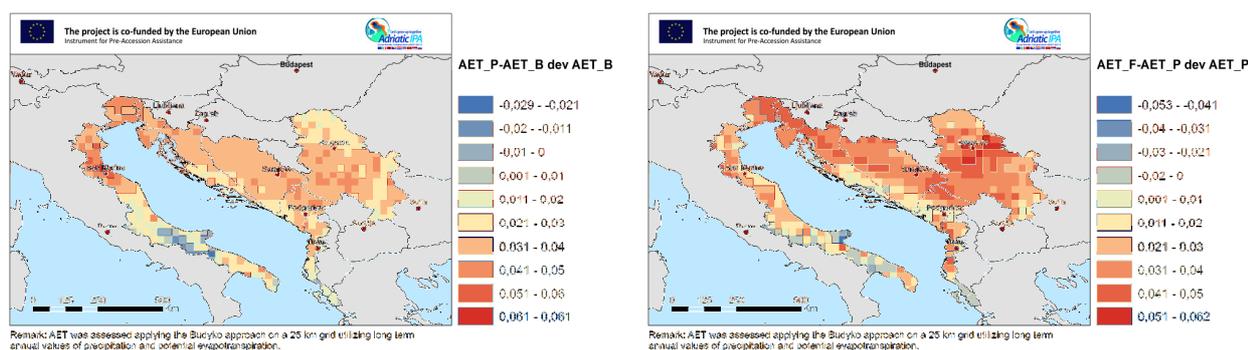
Figure 8: Relative changes of annual actual evapotranspiration between present - base period and future - present period based on mean annual ensemble values of RegCM3, ALADIN and PROMES models.

3.2.5 De Martonne's Index of Aridity

De Martonne's Index of Aridity (see eq. 3) based on the ensemble of RegCM3, ALADIN and PROMES models for baseline, present and future period is presented in Figure 9.

The De Martonne's Index of Aridity show extremely humid areas in the Alps, major parts of Dinarides and part of Apennines. Very humid areas are in Marche region and part od Apennines, in Po basin (N Italy), central Balkan Peninsula (S Croatia, E and W BiH, W Serbia), W Albania and in Corfu. Humid areas are found in bigger part of Serbia, part of Po basin, central E Italy and small part of central Albania, while semi humid areas in Transylvanian Depression (N Serbia) and central E Italy. Semi-dry and dry areas are in SE Italy.

According De Martonne's Index of Aridity in the future the situation will be similar with furher changes: a larger area of the Dinarides will be himid instead of very humid conditions, part of the Apennines, Po basin, SW Albania and Corfu will be semi humid instead of humid and SW Italy even more dry.
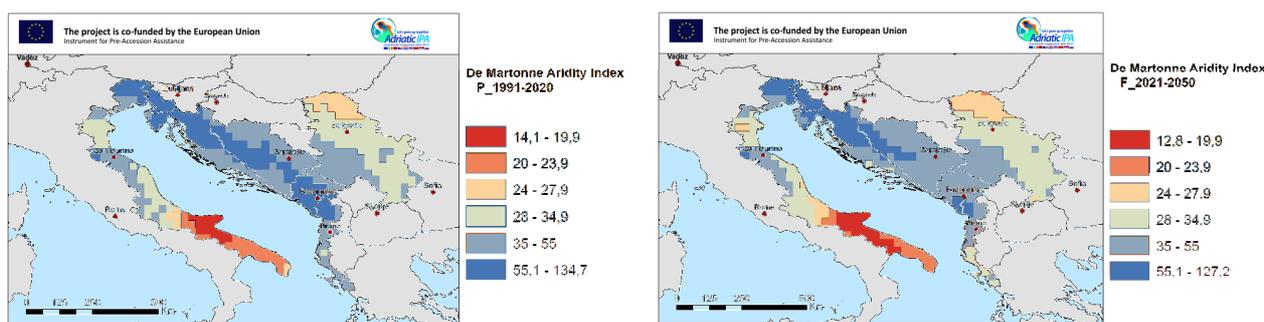
Figure 9: De Martonne's Aridity Index based on mean annual ensemble values of RegCM3, ALADIN and PROMES models for present and future period.

4. WATER RESOURCES VULNERABILITY TO CLIMATE CHANGE

4.1 Water quantity

According to UNEP methodology (2009), vulnerability is a function of water availability, use and management parameters. One of the parameters is **water exploitation index** (WEI) or water stress, which is the ratio of total water demand (domestic, industrial and agricultural) to the available amount of renewable water resources that consists of surface water and groundwater safe yield (river discharge or runoff and groundwater recharge). Values from 0.2 to 0.4 indicate medium to high stress, whereas values greater than 0.4 reflect conditions of severe water limitations (Vörösmarty et al, 2000).

Water demand is estimated as water withdrawal by sectors. Future water demand can be estimated regarding population growth (domestic water use), GDP changes (industrial water use) and land use changes (agricultural water use). Nevertheless, all these are also subject to policy. Future water demand will be assessed applying different scenarios. Uncertainty can be expressed as differences among min, plausible and max values.

Water quantity indicators

Variables and indicators for water quantity sensitivity to CC are presented in Table 2. Water quantity indicators were calculated for the present (P; 1991-2020) and future (F; 2021-2050) periods. As climate data results from CC-Waters project were used (CC-WaterS, 2010; see chapter 3). Climate variables maps are available in spatial resolution of 0.25^{o}, which is approximately 25 km when projected. All climate variables maps present average value for each grid cell for particular period.

Table 2: Variables and indicators for water quantity.

		SYMBOL	UNITS	DATA SOURCES & FORMULAS
VARIABLES	Precipitation	RR	$mm/yr = (l/m^2)/yr$	*CC-WaterS SEE Project (CC-WaterS, 2010)*
	Actual evapotranspiration	AET	$mm/yr = (l/m^2)/yr$	*Budyko method*
	Water demand - total	WD	$mm/yr = (l/m^2)/yr$	WD = DWD + AGRWD + INDWD
	Water demand - domestic	DWD	$(l/m^2)/yr$	EUROSTAT, Partner Countries
	Water demand - agriculture	AGRWD	$(l/m^2)/yr$	Partners countries, FAO, EUROSTAT
	Water demand - industry	INDWD	$(l/m^2)/yr$	EUROSTAT, Partner Countries
INDICATORS	Local Total Runoff	LTR	$mm/yr = (l/m^2)/yr$	LTR = RR – AET
	Local Water Exploitation Index	LWEI	ND	LWEI = WD / LTR
	Local Water Surplus	LWS	$mm/yr = (l/m^2)/yr$	LWS = LTR – WD

Generally all indicators are calculated as long term mean annual values. To account for uneven seasonal distribution of water demand and water availability, a seasonal water exploitation index is additionally considered (see chapter 4.1.3.2 – 4.1.3.4).

DRINK ADRIA

4.1.1 Local total runoff

Water availability was calculated as a simplified water balance:

$$Q = RR - AET + \Delta S \qquad (5)$$

where Q is total runoff (surface and groundwater), RR is precipitation, AET is actual evapotranspiration and ΔS is a storage change term. Since long term annual values are used, the storage term ΔS is neglected.

Calculations of total runoff were elaborated based on grids with spatial resolution of 25 km ($0,25°$). Deficits of the grid by grid calculations exist, since inflowing and outflowing runoff to and out of the cells is not taken into consideration with this approach. The headwaters and upper basins as a source for water supply (e.g. from surface water, bank filtration and regional groundwater systems etc.) are neglected. Basically only direct runoff recharge (from precipitation) was taken into consideration. Based on these considerations, the indicator was named LOCAL TOTAL RUNOF (LTR) instead of water availability. Local total runoff is calculated as:

$$LTR = RR - AET \qquad (6)$$

Precipitation (RR) and actual evapotranspiration (AET) input mean values were obtained from selected RCM's, which has some bias correlations (see chapter 3).

Figure 10 presents baseline, present and future local total runoff. In all periods total runoff is high in the Alps, northern Dinarides and around Skadar lake (border between Montenegro and Albania), whereas in all other parts it is significantly lower, which means very low annual recharge in those areas. The lowest total runoff is in SW part of Italy (especially Puglia region – Gargano Promotory) and N Serbia.
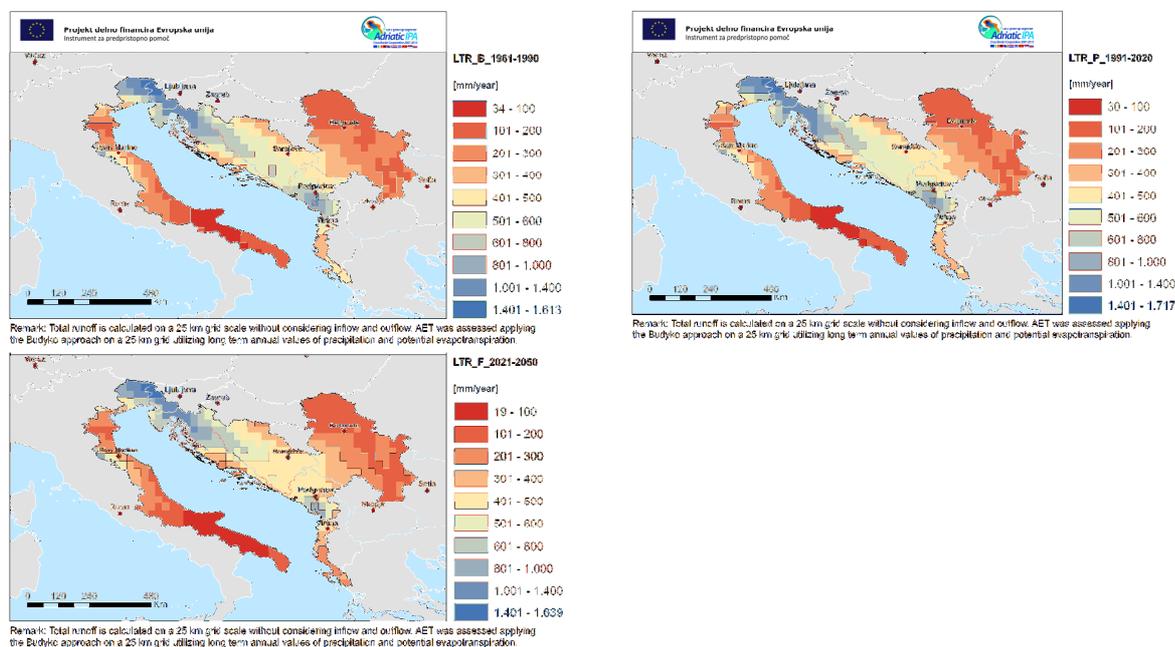
Figure 10: Local total runoff (LTR) based on mean annual ensemble values of RegCM3, ALADIN and PROMES models for baseline (B), present (P) and future (F) period.
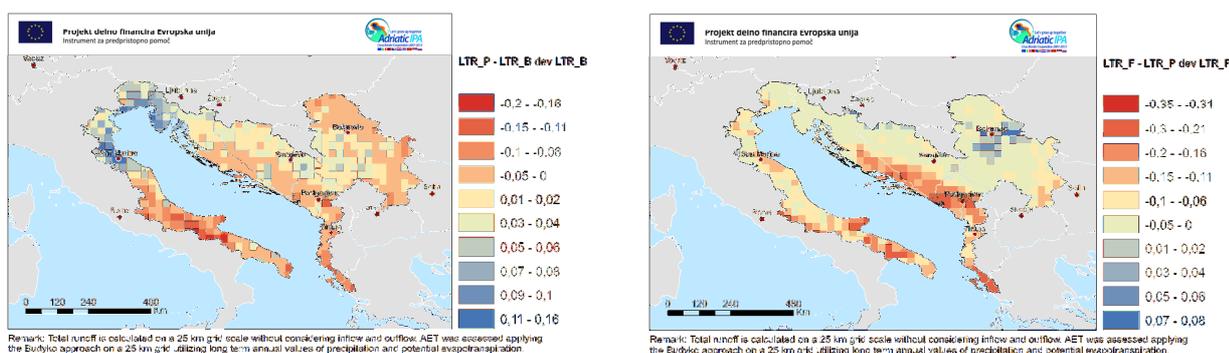
LTR maps were compared to modelled national runoff data. LTR is calculated with as difference between precipitation and AET. Precipitation is underestimated in mountainous areas, whereas AET is underestimated in lowland areas and overestimated in mountainous areas. Consequently, runoff is underestimated in some mountainous areas (Alps, Dinarides, Apennines) and overestimated in some plain areas. LTR is underestimated also in eastern-central Serbia. Due to the coarse spatial resolution (25 km grid) local spatial heterogeneities are however not captured.

Differences between the time periods are very low, therefore the relative changes of absolute values of local total runoff (ΔLTR) were calculated (see equations 4.1 and 4.2). With relative change impact of climate change on local total runoff can be estimated. Relative changes of LTR between present (1991-2020) and base (1961-1990) and between future (2021-2050) and present (1991-2020) period are presented in Figure 11. Present-base comparison show higher LTR (mean more recharge; up to 16 %) N Italy, W Slovenia and Istra Peninsula (Croatia). Lower LTR is observed in central Balkan Peninsula (northern Croatia, SE half of BiH and Montenegro and E Serbia, while for E half of Serbia, W Balkan Peninsula (S and coastal Croatia, W BiH and Montenegro, Albania and Corfu scenarios show the reduction of local total runoff up to 20 %.

Relative changes of LTR between future and present period show that higher LTR in the future would be only in some parts of central Serbia. Conversely, lower LTR (up to 30 %) will be in some parts of SE half of Italy and W Balkan Peninsula (S half of Croatia, SW BiH, W Montenegro, Albania and Corfu). Scenarios for all other areas show smaller reduction of local total runoff.

Generally, scenarios show that there would be up to 30 % less recharge and water available in the future in southern Italy and Greece and around 20 % less recharge in southern Croatia (Dalmatia), southern Serbia and coastal part of Montenegro, whereas in other areas there is no significant change in LTR. Considering 10-20% uncertainty, all other parts of the region are inside this range. Nevertheless, also small regional changes can influence local water supply.

Map of changes in average annual water availability under the LREM-E scenario by 2030 (EEA 2005) shows diminishing of water availability from 5-25 % in southern Italy and Greece. There is no data for Croatia, Serbia, Montenegro and Albania.

Figure 11: Relative change of Local total runoff (ΔLTR) between present - base period and future - present period based on mean annual ensemble values of RegCM3, ALADIN and PROMES models.

DRINK ADRIA

4.1.2 Water demand

Present water demand

Total water demand (WD) was evaluated as the sum of domestic (DWD), agricultural (AGRWD) and industrial (INDWD) water demand:

$$WD = DWD + AGRWD + INDWD. \qquad\qquad (7)$$

All WD data have units m³/year but for further calculations these data were transformed to mm/year (with division by area). Data sets of WD were provided on NUTS 3 level (where data were available) or on country level for individual countries by the project partner. Agricultural water demand was not easy to estimate since most of counties do not have geo-referenced water use data. Moreover, it is not easy to get industrial water use data with separation of water use for hydro power plant and thermal and nuclear PP. Water use for hydro power plant is in some countries very high, but this water use does not present significant water loss and should be excluded.

Not all countries have available data on NUTS 3 level. In such cases country data was used. In this case weights were defined for particular WD in order to allocate country water demand value to NUTS 3 level (Table 3). For domestic water demand (DWD) data weight is population density (population number for each NUTS 3 respectively). Weight for agricultural water demand (AGRWD) is a percentage of agricultural areas in particular NUTS 3 and for industrial water demand (INDWD) is a percentage of industrial areas in particular NUTS 3 area (Table 3). Whereas most of the countries involved in the project are not included with its whole territory in the IPA region (within IPA programme), we collected only data for the eligible parts, all other data were excluded from the further analyses. This is for Italy eastern part of a country, for Slovenia, Croatia and Albania western part and Corfu island in Greece. For BiH just the most eastern part of the country was excluded from this research. In case of Republic of Serbia, which is not involved into EUROSTAT nomenclature system, all data were collected on municipality level. Thus they also provided shape files for further analyses. In table 4 is presented an overview of data levels and collected data sets obtained by IPA partner countries.

Table 3: Methods for estimation of water demand for different sectors in NUTS 3 scale

Scale of data sets	DWD	AGRWD	INDWD
COUNTRY	$Weight = \dfrac{No.\,population\,NUTS\,3}{population\,in\,country}$	$Weight = \dfrac{CLC\,agricultural\,areas\,NUTS\,3}{NUTS\,3\,area}$	$Weight = \dfrac{CLC\,industrial\,areas\,NUTS\,3}{NUTS\,3\,area}$
NUTS 3	Domestic water use [m³/yr] for each NUTS 3	Agricultural water use (irrigation) [m³/yr] for each NUTS 3	Industrial water use [m³/yr] for each NUTS 3
Municipality	Domestic water use [m³/yr] for each Municipality	Agricultural water use (irrigation) [m³/yr] for Municipality	Industrial water use [m³/yr] for each Municipality

Future water demand

For future water demand four scenarios of water demand changes have been applied:

- 10 % decrease of WD,
- no change in WD,
- 10 % increase of WD,
- 25 % increase of WD.

DRINK ADRIA

For calculating water demand in the future, factor ΔWD was introduced:

$$WD_{future} = (DWD + INDWD + AGRWD) * \Delta WD \qquad (8)$$

where ΔWD is 0.9, 1.0, 1.1 and 1.25 for four water demand scenarios in the future.

Domestic water demand

Figure 12 presents domestic water demand for present and future scenarios for DRINKADRIA countries within IPA Adriatic area. It can be clearly seen that data was gathered on NUTS 3 level. In general, the pattern is following the population density. In areas with rugged relief, such as in Alpine / Subalpine areas and valleys (e.g. Po valley), values are overestimated in the mountainous area and underestimated in valleys, because the values were generalized to the whole NUTS3 region.

All presented maps (present and future scenarios) show the same pattern due to the selection of future scenarios. Higher domestic water demand is attached to the plains (i.e. Po plain) and the territories of major cities. Conversely, lower domestic water demand is found in mountainous and less accessible regions.
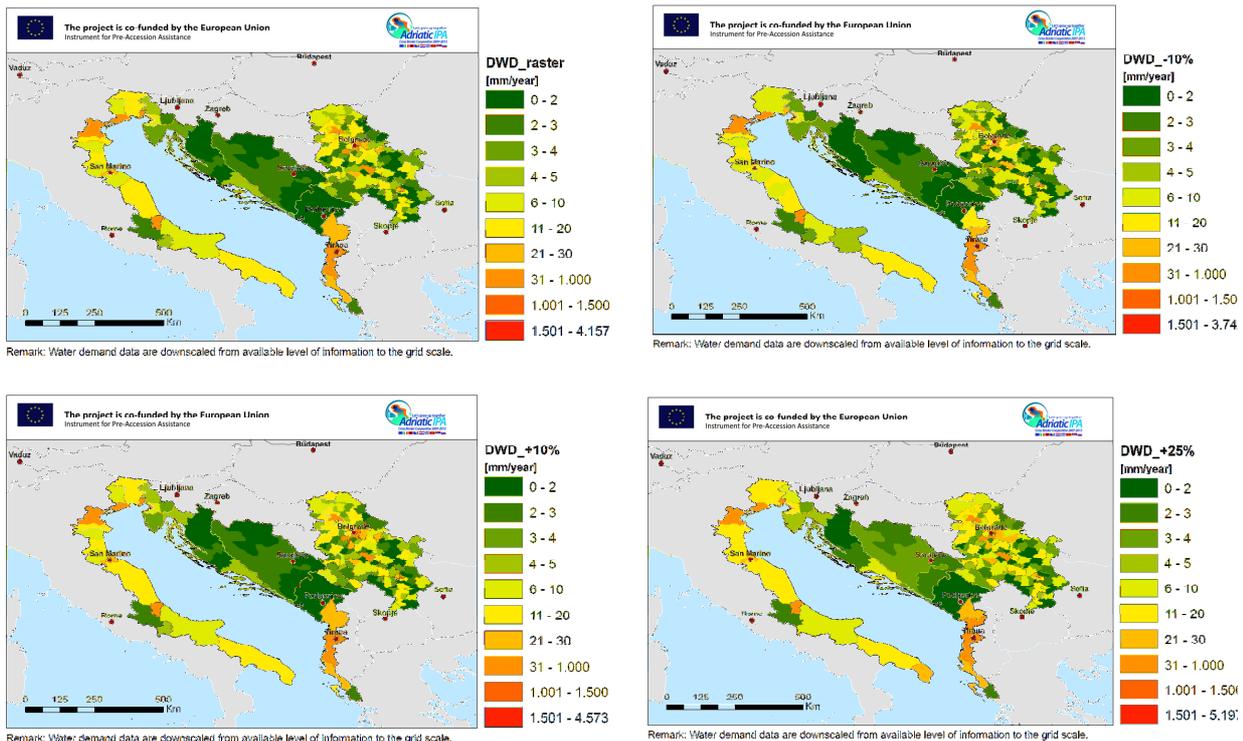
Figure 12: Domestic water demand (DWD) for present and future scenarios for DRINKADRIA countries within IPA Adriatic area.

Agricultural water demand

Figure 13 presents agricultural water demand for present and future scenarios for DRINKADRIA countries within IPA Adriatic area. Very high agricultural water demand is in Corfu and Albania because of irrigation. In Serbia pattern is very scattered due to the data scale on Municipality level. All other counties show very low agricultural water demand.

Figure 13: Agricultural water demand (AGRWD) for present and future scenarios for DRINKADRIA countries within IPA Adriatic area.

Industrial water demand

Figure 14 presents industrial water demand for present and future scenarios for DRINKADRIA countries within IPA Adriatic area. High industrial water demand is in the Po plain and the most southern parts of Italy, in Slovenia (especially the coastal area) and central Serbia. High industrial water demand in Montenegro is due to hydropower plant water demand, which could not be subtracted from the data, therefore this has to be considered in all other results. It should be noted that in areas with rugged relief, such as in Alpine / Subalpine areas and valleys (e.g. Po valley and Friuli Venezia Giulia Region), values are overestimated in the mountainous area and underestimated in valleys, because the values were generalized to the whole NUTS3 region.
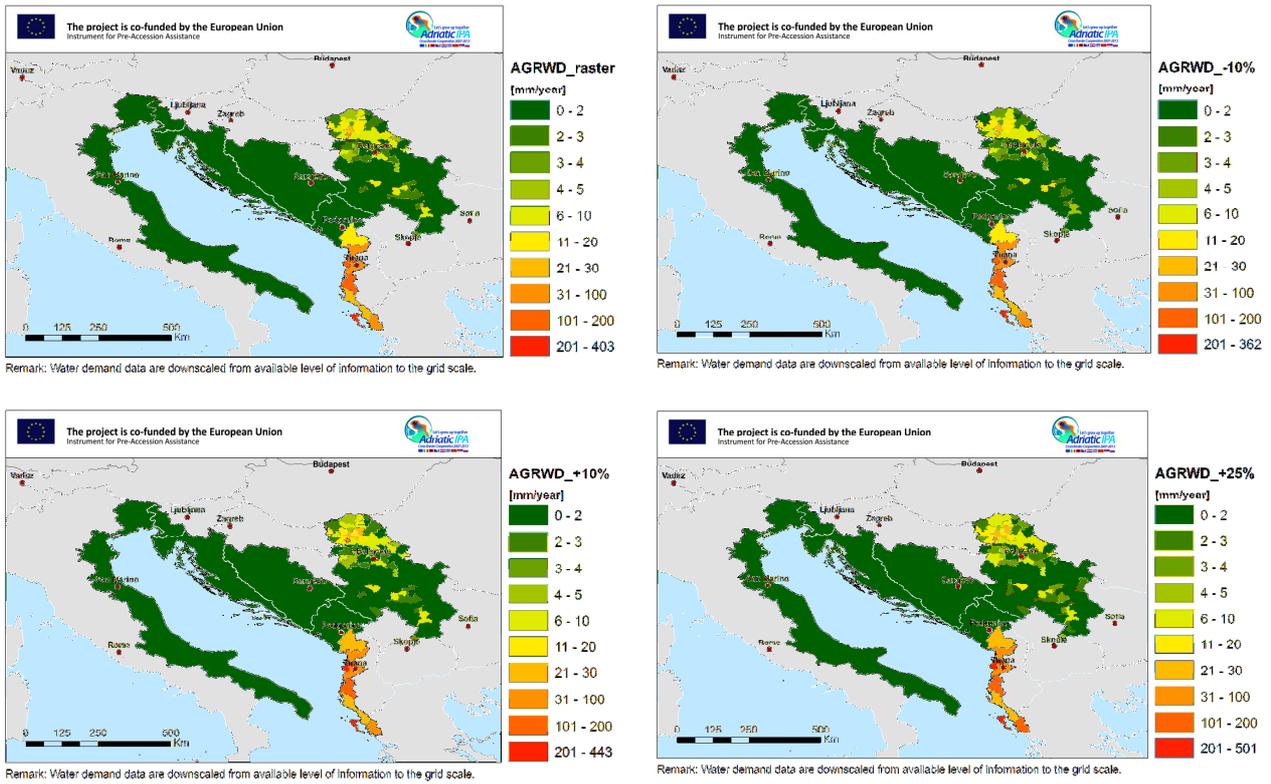

Figure 14: Industrial water demand (INDWD) for present and future scenarios for DRINKADRIA countries within IPA Adriatic area.
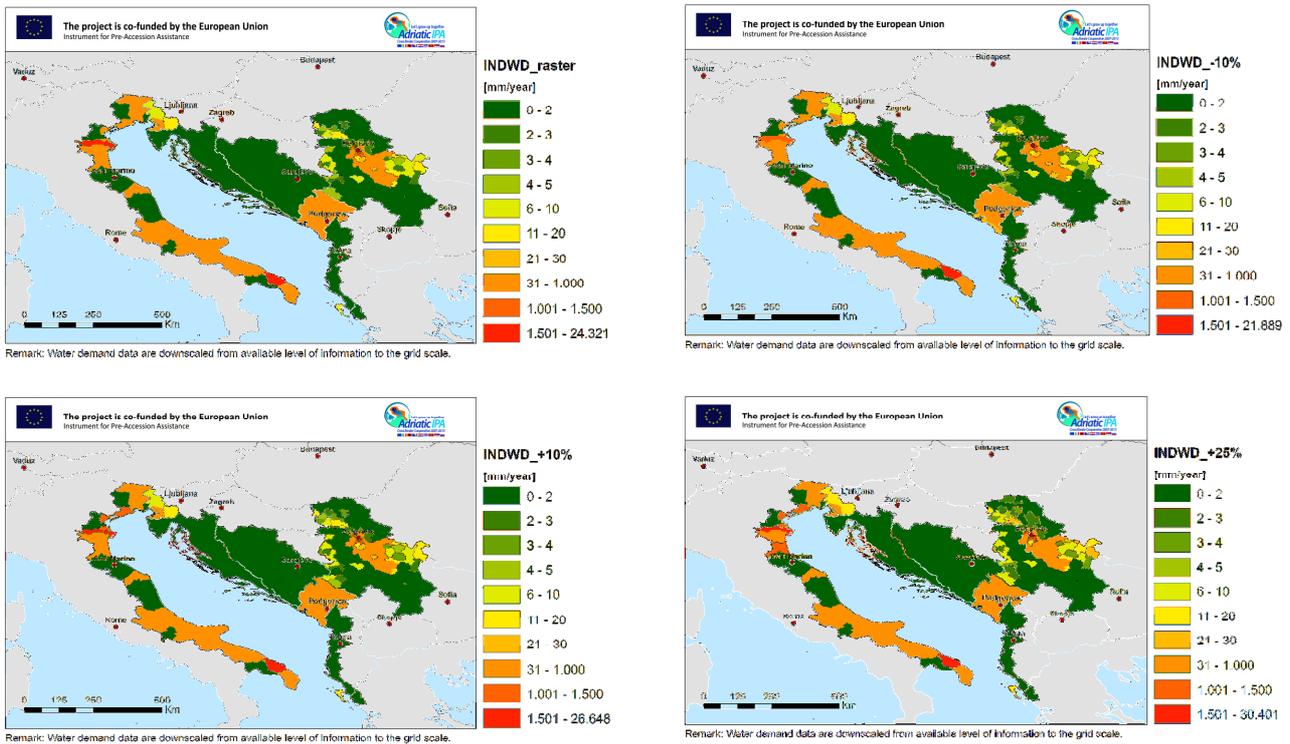
Total water demand

Figure 15 presents total water demand for present and future scenarios for DRINKADRIA countries within IPA Adriatic area. Due to the selection of future scenarios, the pattern for all maps is practically the same. Higher total water demand is in Po plain and SE part in Italy, W Slovenia (especially in coastal area), central Serbia, in Montenegro Albania and Corfu. While high total water demand in Italy, Slovenia, Serbia and Montenegro is the result of higher industrial water demand, in Albania and Corfu is of higher agricultural and domestic water demand.
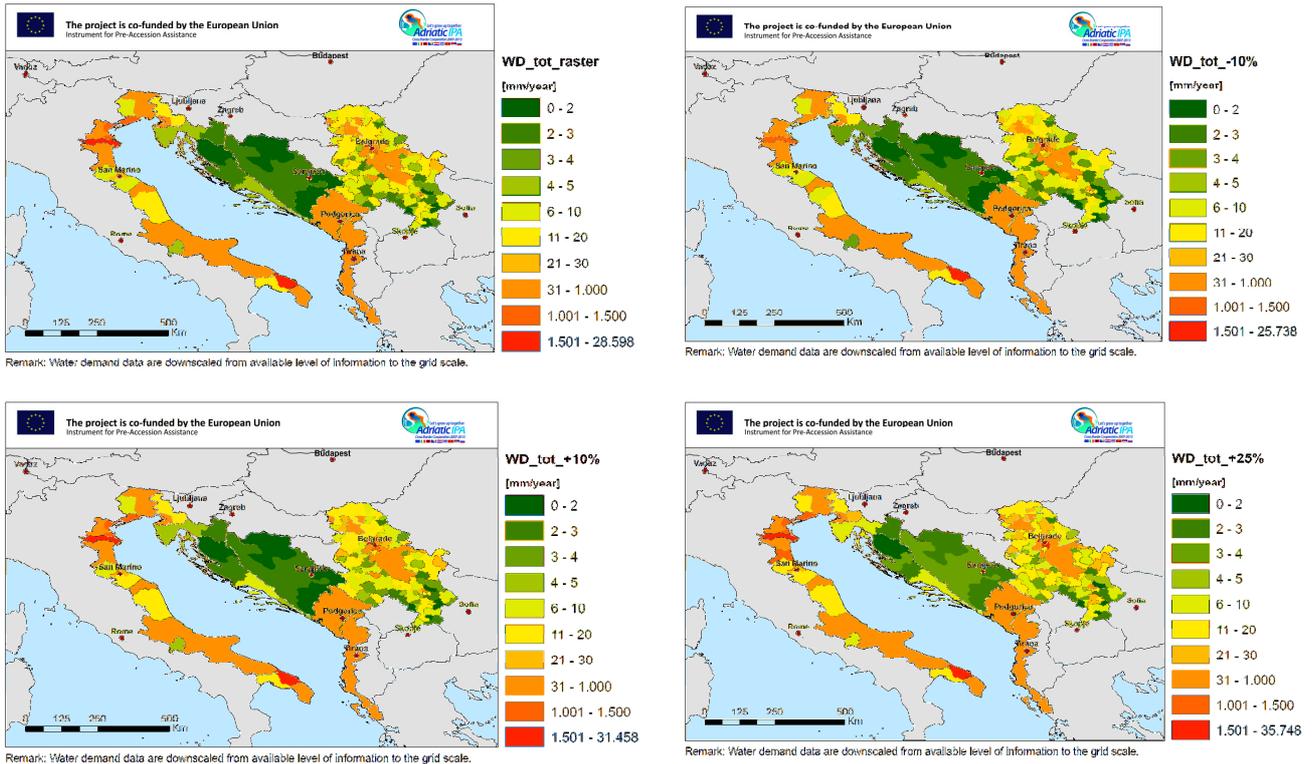
Figure 15: Water demand for present and future scenarios for DRINKADRIA countries within IPA Adriatic area.

4.1.3 Local water exploitation index (LWEI)

From WD maps and LTR maps, local water exploitation index (LWEI) can be calculated as a ratio between annual WD and LTR for all periods and scenarios:

$$LWEI = \frac{WD}{LTR} \tag{9}$$

where LWEI is Local Water Exploitation Index, WD is Water Demand and LTR Local Total Runoff.

The expression 'local' in Local water exploitation index is because total runoff was calculated as direct runoff, not taking into consideration inflowing and outflowing runoff to and out of the $0.25^{o} \times 0.25^{o}$ grid cell.

4.1.3.1 Annual local water exploitation index (LWEIa)

Considering annual values and different sectors contributing to water demand Annual Local Water Exploitation Index ($LWEI_a$) is then:

$$LWEI_a = \frac{WD_a \cdot \Delta WD}{LTR_a} = \frac{(DWD + AGRWD + INDWD) \cdot \Delta WD}{RR_a - AET_a} \tag{10}$$

with

WDa ... annual water demand [$l/m^2/yr = mm/yr$],
LTRa ... annual local total runoff [mm/yr],
ΔWD ... factor for change of WD in future scenarios (0.9, 1.0, 1.1, 1.25),
DWD ... domestic water demand [$l/m^2/yr = mm/yr$],
AGRWD ... agricultural water demand [$l/m_2/yr = mm/yr$],
INDWD ... industrial water demand [$l/m_2/yr = mm/yr$],
RRa ... mean annual rainfall [mm/yr],
AETa ... mean annual actual evapotranspiration [mm/yr].

Local Water Exploitation Index values were classified into five stress classes:

< 0.2 very low water stress
0.2 – 0.4 low water stress
0.4 – 0.6 medium water stress
0.6 – 0.8 high water stress
> 0.8 very high water stress.

Values above 0.4 already signify severe water stress and measures for diminishing of water stress have to be considered and applied.

The results (Figure 16) show medium water stress in central and SE Italy, in some places of central Serbia, NE part of Montenegro and central Albania. High and very high water stress on annual level is in Po plain and southern half Italy, in Karst region of Slovenia, in central Serbia and Corfu. Scenarios for the future show the same pattern, only areas with severe (medium, high and very high) stress are supposed to be larger.

DRINK ADRIA

The resulting maps with regions with high stress are actually indicators for measures to be applied in these areas. These measures are discussed together with annual LWEI considering seasonality (LWEI$_{asw}$; see chapter 4.1.3.4).

Similarly, Flörke et al. (2011) show severe water stress (more than 0,4) for present state in central and south Italy and north-east Greece. They used different future scenarios for projection to 2050 (Economy First Scenario and Sustainability Eventually Scenario). The first one shows sever water stress in the most part of Italy, south-east Serbia, central Albania and eastern Greece, whereas the second one is milder and show only some areas with severe stress in Italy and Greece (Flörke et al. 2011, EEA 2012c). Differences are due to different scenarios and lower resolution (simulations based on river basin).
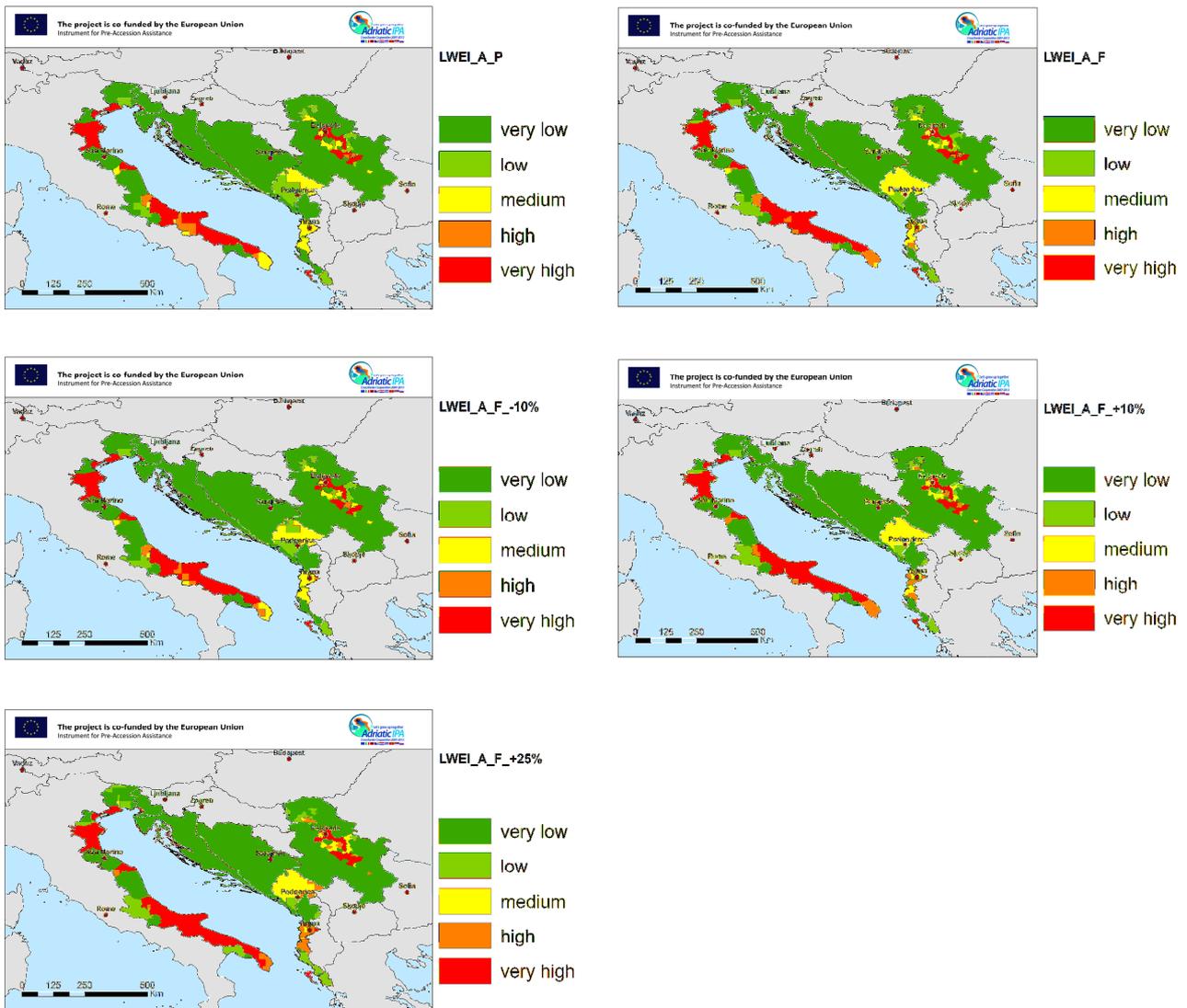
Figure 16: Annual Local Water Exploitation Index (LWEIa) for present and future scenarios of water demand for DRINKADRIA countries within IPA Adriatic area.

Assessing the LWEI$_a$ on an annual basis neglects seasonality and extremes in demand and availability. These factors are however frequent causes for water scarcity and need to be addressed. Figure 17 and Figure 18 schematically illustrate this problem.
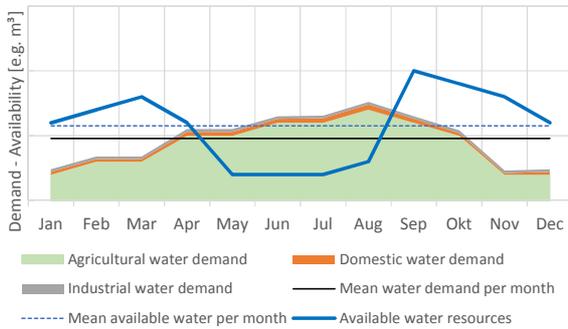
Figure 17: Hypothetical example of monthly water demand and availability.
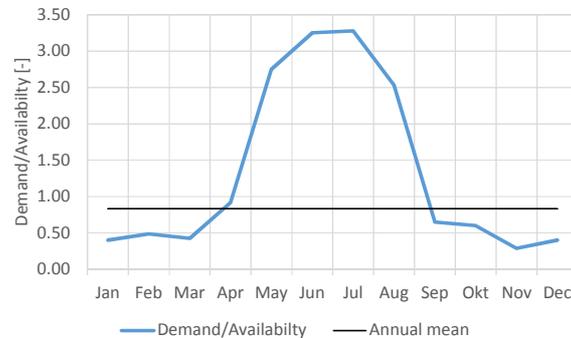
Figure 18: Demand to availability ratio of a hypothetical example

Assessing the LWEI$_a$ on an annual basis would show no substantial deficits, as the mean water demand is lower than availability (solid and dashed line in Figure 17). This fact is also visible in Figure 18, where the annual mean ratio between demand and availability is lower than 1. The hypothetical example in Figure 18 however shows, that in single months the demand is higher than the availability, leading to ratios between demand and availability larger than 1 (Figure 18).

For this reason it was decided to evaluate the LWEI for three different time periods:

(i)   annual basis (LWEI$_a$),

(ii) summer period (April – September) – LWEI$_s$ and

(iii) winter (October – March) period – LWEI$_w$.

As a basis for further assessments within DRINKADRIA project, the LWEI of the different time periods was combined to final Local Water Exploitation Index (LWEI$_{asw}$). The methodology for the assessment of the summer and winter LWEI (LWEI$_s$, LWEI$_w$) is described in the following sections. The procedure for estimating actual evapotranspiration for summer and winter period, which is needed for the water availability term, is described beforehand.

4.1.3.2   LWEI for summer season (LWEIs)

The Local Water Exploitation Index for summer season (LWEI$_s$) is estimated as the ratio between water demand and availability (total runoff) in summer months. The months of April to September are thereby included. Similar to the annual LWEI$_a$, a multiplicative factor ΔWD for considering water demand change in future is also used, which is set to 1 for the recent period (1991-2020). To account for an increase in domestic water demand in summer months, e.g. due to tourism, a water demand seasonality index (α_{sD}) is introduced and provided by project partners. It is defined as the ratio between domestic water demand in summer with regard to winter season. The domestic water demand is then:

$$DWD = DWD_w + DWD_s = DWD_w + DWD_w \cdot \alpha_{sD} = DWD_w \cdot (1 + \alpha_{sD}) \qquad (10)$$

$$DWD_W = \frac{DWD}{1+\alpha_{sD}} \tag{11}$$

$$DWD_s = DWD \cdot \left(1 - \frac{1}{1+\alpha_{sD}}\right) = DWD \cdot \left(\frac{\alpha_{sD}}{1+\alpha_{sD}}\right) \tag{12}$$

with

α_{sD} as domestic water demand seasonality index (a ratio between domestic water demand in summer months with regard to winter months), DWD_s domestic water demand in summer and DWD_w domestic water demand in winter.

For agricultural water demand it was assumed that the most water for agriculture (irrigation) is consumed in summer season, therefore annual value of agricultural water demand was taken into account. For industrial water demand it is assumed that it is the whole year more or less constant, therefore in summer season industrial water demand is a half of annual industrial water demand. Consequently, total water demand in summer is:

$$WD_s = DWD \cdot \left(\frac{\alpha_{sD}}{1+\alpha_{sD}}\right) + AGRWD + 0.5 \cdot INDWD \tag{13}$$

The Summer Local Water Exploitation Index (LWEI$_s$) is calculated as

$$LWEI_s = \frac{WD_s \cdot \Delta WD}{\max(LTR_s, 0.1)} \tag{14}$$

with

$LWEI_s$ - water exploitation index for summer season (Apr- Sept)
WD_s - water demand in summer season
LTR_s - local total runoff in summer season; calculated LTR$_s$ in summer (PP$_s$-AET$_s$) can be less than 0, therefore 0.1 mm is set to be the lowest value
ΔWD - factor for change of WD in future scenarios (0.90, 1.00, 1.10, 1.25)
DWD - domestic water demand
$AGRWD$ - agricultural water demand
$INDWD$ - industrial water demand

The water availability (local total runoff) is calculated as the difference between summer precipitation and AET in summer months:

$$LTR_s = RR_s - AET_s \tag{15}$$

with

LTR_s - local total runoff in summer season
AET_s - mean annual actual evapotranspiration for summer season
RR_s - mean summer rainfall

The Budyko formula only estimates mean annual AET values. To estimate summer AET$_s$, annual AET$_a$ was multiplied with a scaling factor (β_{sA}). It is the ratio between PET in summer months and

on an annual basis. Furthermore, AET_s was limited to the amount of summer rainfall, since AET cannot be larger than available summer rainfall. AET_s for summer months is calculated as follows:

$$AETs = min(AETa \cdot \beta sA, RR_s) \qquad (16)$$

$$\beta_{sA} = \frac{PET_s}{PET_a} \qquad (17)$$

with

β_{sA} – scaling factor for actual evapotranspiration for summer season
PET_a - mean annual potential evapotranspiration
PET_s - mean summer potential evapotranspiration

The approach for estimating summer AET assumes that the ratio between summer and annual AET is similar to the ratio between summer and annual PET. This approach is feasible, since the seasonal distribution of AET is similar to (scaled) PET. However water availability may limit the AET value, which was explicitly considered in the above equation.

The results of $LWEI_s$ are presented on Figure 19 where generally only two extreme classes of $LWEI_s$ for summer season appear: either very low or very high stress. A very high water stress in summer months is in practically the whole E Italy, except in small part of Appenines and the Alps, on Karst Plateau in Slovenia, SW Croatia, SW and partly N of BiH, a large part of Serbia, except the west, in Montenegro, Albania and Corfu.Very low water stress occur in Alps and northern Dinarides, part of Appenines (W of San Marino) and western Serbia. There are only few small areas of medium water stress for summer season: small parts of Po plain, in central Croatia, N Albania and individual parts of Serbia. The maps show the same pattern in the future with generally even higher stress in some regions.

$LWEI_s$ for summer months present **the worst case scenarios regarding water stress**, which are very important in water resources management, since in summer season water demand is much higher and droughts are more frequent in the last decades.

The resulting maps are actually indicators for measures to be applied in a region with high stress. These measures are discussed together with annual LWEI considering seasonality ($LWEI_{asw}$; see chapter 4.1.3.4).
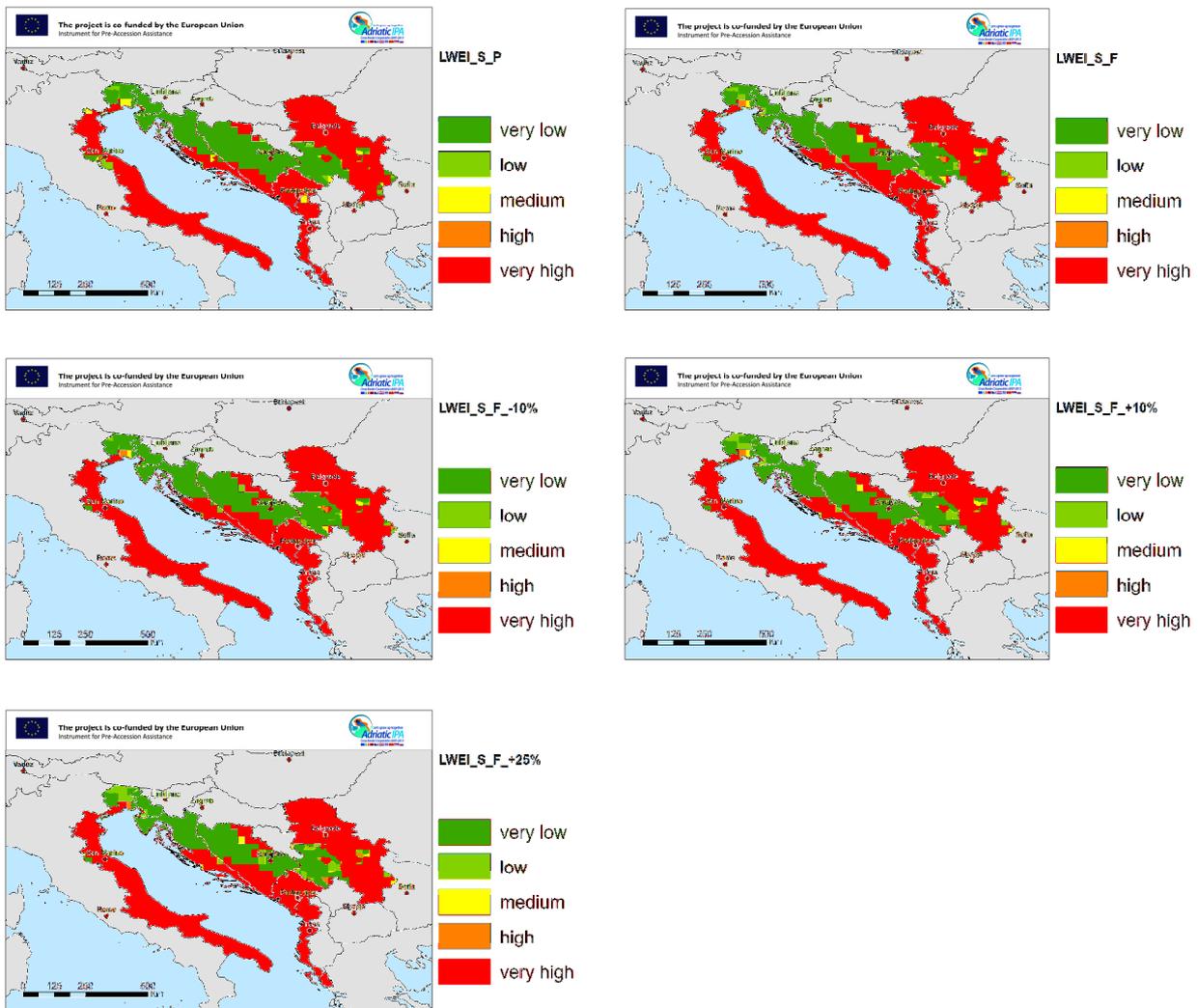
DRINK ADRIA

Figure 19: Summer Local Water Exploitation Index (LWEIS) for present and future scenarios of water demand for DRINKADRIA countries within IPA Adriatic area.

4.1.3.3   LWEI for winter season (LWEIw)

The winter Local Water Exploitation Index (LWEI$_w$) for the months October to December and January to March is calculated in similar manner compared to the summer value:

$$LWEI_w = \frac{WD_w * \Delta WD}{max(LTR_w, 0.1)} \tag{18}$$

with

LWEI$_w$ - water exploitation index for winter season (Jan to Mar, Oct to Dec)
WD$_w$ - water demand in winter season
LTR$_w$ - water availability in winter season
ΔWD - factor for change of WD in future scenarios (0.90, 1.00, 1.10, 1.25)

For agricultural winter water demand it is assumed that there is no water consumption (no irrigation). For industrial water demand it is assumed that it is the whole year more or less constant, therefore in winter season industrial water demand is a half of annual industrial water demand. Winter water demand (WD_w) is then:

$$WD_w = \frac{DWD}{1 + \alpha_{sD}} + 0.5 \cdot INDWD \qquad (19)$$

with

DWD – domestic water demand
$INDWD$ – industrial water demand
α_{sD} – domestic water demand seasonality index (increase of domestic water demand in summer months with regard to winter months).

The water availability (local total runoff) is calculated as the difference between winter precipitation and AET in winter months:

$$LTR_w = RR_w - AET_w \qquad (20)$$

with

LTR_w – local total runoff in winter season
AET_w – mean annual actual evapotranspiration for winter season
RR_w – mean winter rainfall

Winter AET is calculated as the difference between annual and summer AET:

$$AETw = AETa - AETs \qquad (21)$$

The results of $LWEI_w$ are presented in Figure 20 and show very similar pattern in winter months comparing to annual $LWEI_a$. Generally in the winter the water stress is slightly lower, which is due to higher water recharge in winter months and lower water demand (no agricultural water use and smaller domestic water use in touristic areas). Areas with high water stress occur in the Po plain and southern Italy, in Karst Palteau in Slovenia, and same areas in contral Serbia (around Belgrade). Maps for the future show the same pattern with slightly larger areas of severe water stress (medium, high and very high water stress).

The resulting maps are actually indicators for measures to be applied in a region with high stress. These measures are discussed together with annual LWEI considering seasonality ($LWEI_{asw}$; see chapter 4.1.3.4).
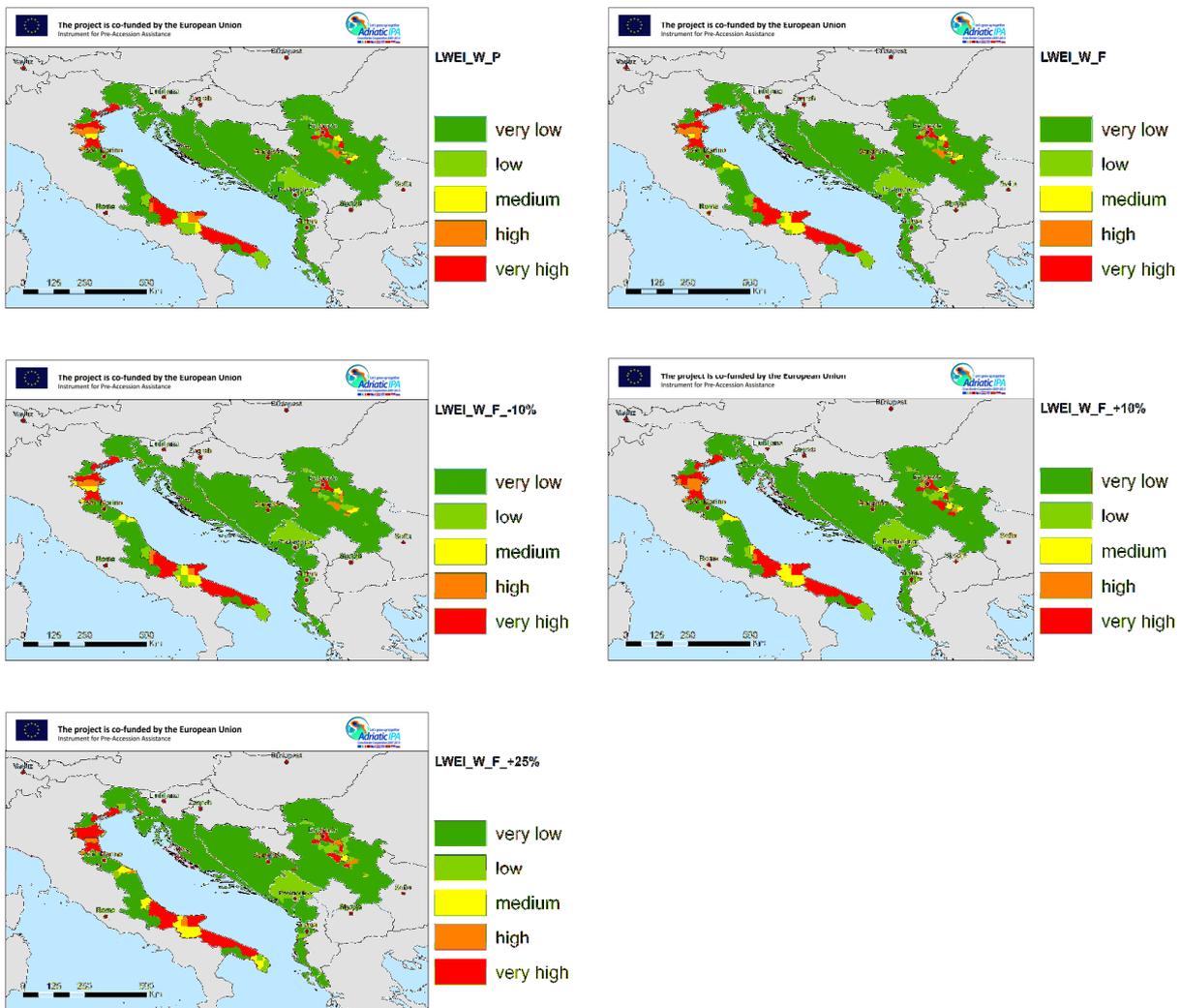
DRINK ADRIA

Figure 20: Winter Local Water Exploitation Index (LWEIw) for present and future scenarios of water demand for DRINKADRIA countries within IPA Adriatic area.

4.1.3.4 Annual Local Water Exploitation index corrected for seasonality (LWEIasw)

For the further evaluation of water resources in the context of DRIANKADRIA project a single annual value resembling of the water quantity sensitivity is needed. After the intersection of winter $LWEI_w$ and summer $LWEI_s$ to a single seasonal value, a matrix is used to derive the Local Water Exploitation Index ($LWEI_{asw}$), utilizing the seasonal and annual $LWEI_a$ values.

To combine the winter and summer LWEI to a seasonal value ($LWEI_{sw}$), the following procedure is applied, assuming that the more critical value in respect to water exploitation is relevant:

$$LWEI_{sw} = max\,(LWEI_s, LWEI_w) \tag{22}$$

Annual water stress (LWEI$_a$) was corrected with seasonal water stress (LWEI$_{sw}$) in order to obtain annual water stress considering seasonality (LWEI$_{asw}$). The method is based on expert classification (Table 4). The classification in Table 5 reflects the fact that higher annual sensitivity leads to high overall sensitivity values, since the overall water budget is limited. Higher seasonal values can on the other hand be compensated by lower annual sensitivity values, as technical measure, e.g. dams and reservoirs can enable a seasonal redistribution of water resources.

Table 4: LWEIasw: Annual Local Water Exploitation Index (LWEIa) considering seasonality (LWEIsw)

			LWEI$_a$				
			very low [0-0.2]	low [0.2-0.4]	medium [0.4-0.6]	high [0.6-0.8]	very high [>0.8]
			1	2	3	4	5
LWEI$_{sw}$	very low	A	A1	A2	A3	A4	A5
	low	B	B1	B2	B3	B4	B5
	medium	C	C1	C2	C3	C4	C5
	high	D	D1	D2	D3	D4	D5
	very high	E	E1	E2	E3	E4	E5

LWEI$_{asw}$				
very low	low	medium	high	very high

On Figure 21 annual LWEI$_{asw}$ considering seasonality is presented, showing a similar pattern as annual LWEI$_a$ with reflecting summer LWEI$_s$. High or very high water stress is in the whole E Italy, except in small part of Apennines and the Alps, on Karst Plateau in Slovenia, in SW Croatia, SW and partly N of BiH, a large part of Serbia, except the west, in Montenegro, Albania and Corfu. Very low water stress occurs in Alps and Dinarides, part of Apennines (W of San Marino) and western Serbia. There are only few small areas of medium water stress: parts of Po plain, in central Croatia, N Albania and individual parts of Serbia. In the future, the pattern will be the same with small changes of LWEI$_{asw}$, more areas with very high stress.

The applied methodology for determination of water stress was based on estimation of the water balance for single grid cell (25 km), in which river inflow is not considered. In most of the areas with high water stress, rivers are already used for irrigation or other purposes. In final water stress maps (Figure 21) major rivers are presented, showing that in grid with high stress surface water can be used, but one has to be aware that rivers are also limited resource.

Due to large scale of the study, results have to be considered with due reservation and as indicator. The resulting maps are actually indicators for measures to be applied in a region with high water stress. In some cases, measures have already been applied.

For example, in Serbia Belgrade does not have problems with water quantity due to Sava riverbank filtration; whereas some other regions in Serbia have already problems with water quantity and will have greater in the future.

Another example is Trieste province in Italy, which has medium water stress and high water stress in the Trieste city area due to very high population density, but in reality the water stress is lower

DRINK ADRIA

and almost not present due to huge water storage in large porous aquifer of Soča/Isonzo Low Plain, which is used for water supply for Trieste province. This is the case also for Po Plain in Italy, which has high water stress, but the actual quantity status is good due to the large volume of water stored in large confined porous aquifer in the Po plain. These porous aquifers make the area resilient to large exploitation. Nevertheless, the LWEI map highlights critical exploitation indexes in the alluvial fans located at transition area between NE Apennines and the Po river plain. This is consistent with an observed bad water quantity status in some of these aquifers that is mainly due to past and present overexploitation.
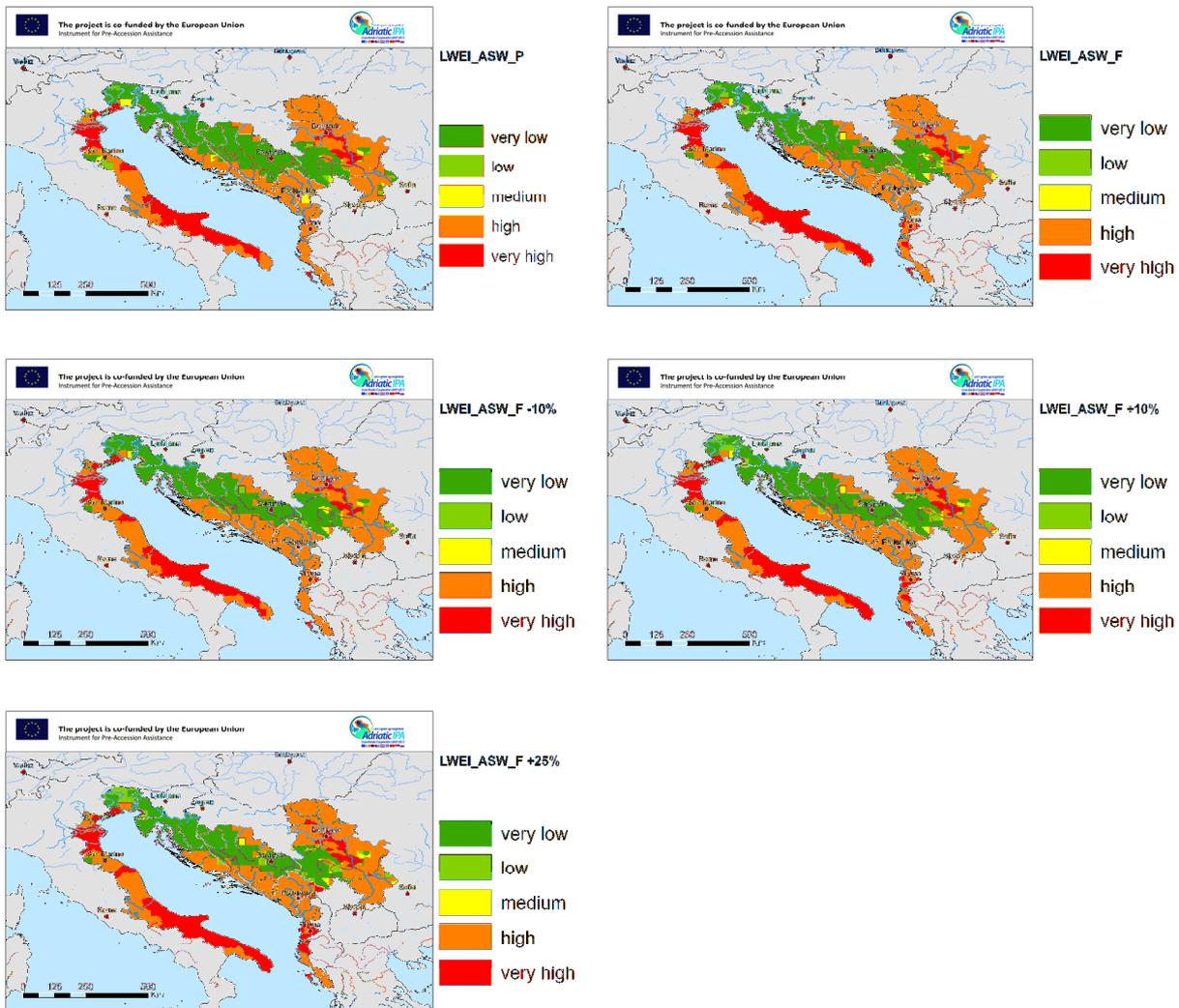
Figure 21: Annual Local Water Exploitation Index considering seasonality (LWEIasw) for present and future scenarios of water demand for DRINKADRIA countries within IPA Adriatic area.

EEA (2015) study is showing high water stress in southern Italy for present and future. For northeastern Italy and Slovenia there is low water stress for present and future. Most of other parts of Italy there is medium water stress. There is no data for Croatia, Serbia, Montenegro and Albania. Similarly, Flörke et al. (2011) show severe water stress (more than 0,4) for present state

in central and south Italy and north-east Greece. They used different future scenarios for projection to 2050 (Economy First Scenario and Sustainability Eventually Scenario). The first one shows sever water stress in the most part of Italy, south-east Serbia, central Albania and eastern Greece, whereas the second one is milder and show only some areas with severe stress in Italy and Greece (Flörke et al. 2011, EEA 2012c). Differences are due to different scenarios and lower resolution (simulations based on river basin).

4.1.3.5   Local Water Surplus (LWS)

Annual local surplus of water resources is calculated as the difference of local total runoff and water demand:

LWS = LTR– WD   (23)

Similarly to LWEI, LWS for the future is calculated for all scenarios of Water Demand (no change, -10 %, +10 %, +25 %).

Annual local surplus of water resources (LWS) for baseline and present period is presented in Figure 22 and for different water demand scenarios in Figure 23. For most of the territory involved in the DRINKADRIA project the water surplus has positive values. The highest water surplus are linked to the Alps, Dinarides and Apennines. High LWS is also in W and SE part of Serbia and central and S Albania. Low water deficit occur only in southern half of Italy, on the Po plain and around Belgrade and some scattered areas in central Serbia. This is mostly due to higher water demand in those areas. In the future the pattern of LWS will be the same, with only slightly increasing of water deficit in some areas.

There are some areas, where water deficit is indicated because of low local total runoff and high water demand, due to large aquifers in the areas, which are used for public water supply. Therefore, the resulting maps are indicators for measures to be applied in a region with water deficit. These measures are discussed together with annual local water exploitation index considering seasonality (LWEI$_{asw}$; see chapter 4.1.3.4).
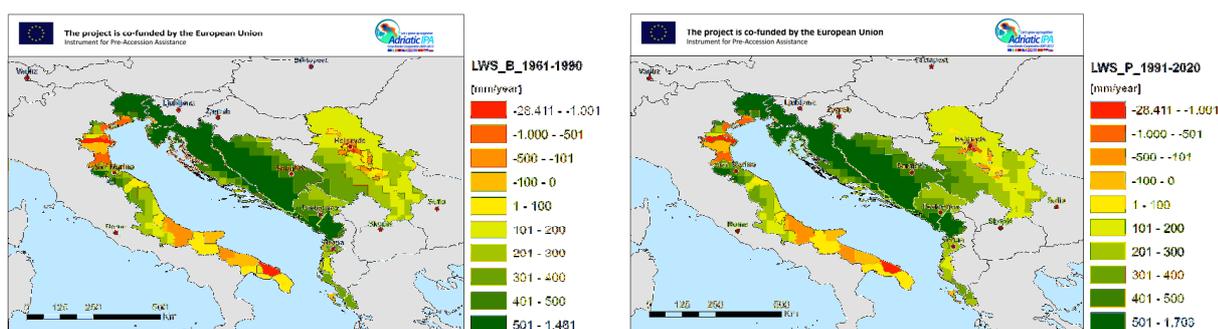
Figure 22: Annual local surplus of water resources (LWS) for baseline and present for DRINKADRIA countries within IPA Adriatic area.
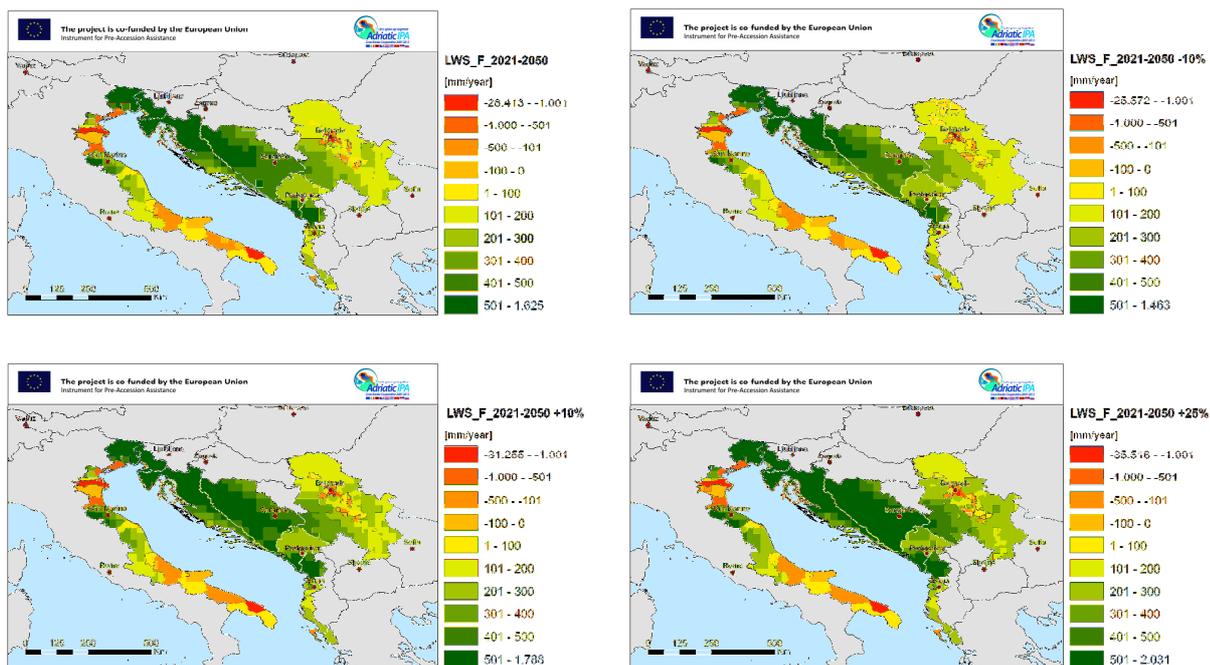
Figure 23: Annual local surplus of water resources (LWS) for future with different water demand scenarios for DRINKADRIA countries within IPA Adriatic area.

4.2   Water quality

Quality problems may occur due to pollution caused by human activities or natural conditions (geological settings). The indicator is "water pollution index" describing the tendency or likelihood for pollutants to reach water resources.

An important driver (exposure in Figure 1) for water quality vulnerability is land use. CORINE data base provides information necessary for the evaluation of the existing land use and estimation of potential pollution load for water resources, which is essential for determining critical areas and consequently for prioritising activities needed for the sustainable management of water resources in the IPA Adriatic area. Applied data set for land use in DRINKADRIA project is Corine Land Cover (CLC2006).

Water quality indicators

Main driver for water quality vulnerability is land use. Impact of land use on water quality is expressed with land use load coefficients (Table 6), which are estimated for each particular land use (CLC level 3) and present potential for pollution. Pollution load index for surface water is a sum of particular land use load coefficient multiplied by the particular land use area (CLC AREA in Table 5). Normalized Pollution load index is indicator for surface water quality – Water quality index SW (WQI_{SW}). Ground water quality indicators are a function of pollution load and effective infiltration coefficient. The latter depends on hydrogeological characteristics of sediments and rocks, which define aquifer type. Therefore HG factor is introduced. HG factor is expressed as effective infiltration coefficient, which was determined according to the International Hydrogeological Map of Europe (BGR & UNESCO 2014). Multiplying Surface water quality index (WQI_{SW}) with HG factor and normalizing we obtain indicator for groundwater quality - Water quality index GW (WQI_{GW}). The methodology for the assessment of the surface and groundwater quality index was developed within the CC-WARE project (CC-WARE, 2014a) and is described in the following sections.

No indicators were calculated for the baseline time period (B; 1961-1990), since no comprehensive data sets for land use (CLC), covering the whole IPA area, exist. Furthermore, after the major political changes in the 1990's in the IPA ADRIATIC area, some water demand parameters changed significantly.

Table 5: Variables and indicators (red rows) for water quality.

INDICATORS	SYMBOL	UNITS	DATA SOURCES & FORMULAS
Land use load coefficients	LUSLI	Non dimensional	land use load coefficients for particular land use – literature
Pollution load index	PLI	Non dimensional	Normalized LUSLI
Water quality index SW	**WQI_{SW}**	**Non dimensional**	**(PLI_j · CLC $AREA_j$) and normalized from 0 to 1**
HG factor	HG	Non dimensional	HG factor according to IHME map categories
Water quality index GW	**WQI_{GW}**	**Non dimensional**	**(WQI_{SW} · HG) and normalized from 0 to 1**

3.2.1 Present potential pollution load (exposure of water resources to land use impacts) and Surface water quality index (WQI$_{SW}$)

The core data set for the calculation of WQI Index is the CORINE land use data set for 2006 (CLC, 2006) except for Greece where CORINE 2000 (CLC, 2000) is used as 2006 data set is not available. CLC scale is 1:100 000, which corresponds to 1km grid.

For each CORINE land use class at LEVEL 3 an overall water pollution load index is assumed to be proportional to nutrient export coefficients from a given land use in CORINE. Nitrogen and Phosphorous export coefficients have been widely used for assessing the nonpoint sources of pollution in the past. On the basis of the literature review and expert knowledge for each CORINE land use class an appropriate Pollution load index (PLI) has been assigned (see Table 6). To evaluate this concept the relative ranking after normalization of the assigned Pollution load Index (LUSLI) is compared to the phosphorous export coefficients from the literature. Figure 24 shows a plot of the Normalized pollution load index (PLI) and the normalized phosphorous export coefficients for a given CORINE land use classes from literature. Only those CORINE Land uses are shown, for which literature data is available. The data used (Wochna et al., 2011) is shown in Table 7.

Table 6: CORINE Land use and land use load coefficients.

CLC CODE	CLC Description	VERSION 1 Upper range of values from literature *Expert interpretation of literature data LUSLI$_i$ - Relative index of pollution Load_2006 (or Nitrogen Export Coefficients)	VERSION 2 Lower range of values from literature *Expert interpretation of literature data LUSLI$_i$ - Relative index of pollution Load_2006	*Adopted for CC WARE Version 2 - Normalized between 0 and 1 PLI$_i$ -Normalized Index of pollution Load_2006
111	Continuous urban fabric	7	6	0.400
112	Discontinuous urban fabric	6.3	5.5	0.367
121	Industrial or commercial units	8	5	0.333
122	Road and rail networks and associated land	5.5	7.5	0.500
123	Port areas	7	7	0.467
124	Airports	7	7	0.467
131	Mineral extraction sites	9	9	0.600
132	Dump sites	14	14	0.933
133	Construction sites	7	7	0.467
141	Green urban areas	3.5	3.5	0.233
142	Sport and leisure facilities	4	4	0.267
211	Non-irrigated arable land	12	12	0.800
212	Permanently irrigated land	15	15	1.000
213	Rice fields	13.5	13.5	0.900
221	Vineyards	6	6	0.400

DRINK ADRIA

CLC CODE	CLC Description	VERSION 1 Upper range of values from literature *Expert interpretation of literature data	VERSION 2 Lower range of values from literature *Expert interpretation of literature data	*Adopted for CC WARE Version 2 - Normalized between 0 and 1
		$LUSLI_i$ - Relative index of pollution Load_2006 (or Nitrogen Export Coefficients)	$LUSLI_i$ - Relative index of pollution Load_2006	PLI_i -Normalized Index of pollution Load_2006
222	Fruit trees and berry plantations	5	5	0.333
223	Olive groves	4.5	4.5	0.300
231	Pastures	3.5	3.5	0.233
241	Annual crops associated with permanent crops	9	9	0.600
242	Complex cultivation patterns	8.3	8.3	0.553
243	Land principally occupied by agriculture, with significant areas of natural vegetation	4	5.5	0.367
244	Agro-forestry areas	3	3	0.200
311	Broad-leaved forest	3.6	3.6	0.240
312	Coniferous forest	2.5	2.5	0.167
313	Mixed forest	2.8	2.8	0.187
321	Natural grasslands	2.5	2.5	0.167
322	Moors and heathland	2.7	2.7	0.180
323	Sclerophyllous vegetation	2.5	2.5	0.167
324	Transitional woodland-shrub	2.6	2.6	0.173
331	Beaches, dunes, sands	2.5	2.5	0.167
332	Bare rocks	1.5	1.5	0.100
333	Sparsely vegetated areas	2	2	0.133
334	Burnt areas	5	5	0.333
335	Glaciers and perpetual snow	0.1	0.1	0.007
411	Inland marshes	2.3	2.3	0.153
412	Peat bogs	2.3	2.3	0.153
421	Salt marshes	2.3	2.3	0.153
422	Salines	2.3	2.3	0.153
423	Intertidal flats	3	3	0.200
511	Water courses	3	3	0.200
512	Water bodies	3	3	0.200
521	Cooastal Lagoons	3	3	0.200
522	Estuaries	3	3	0.200
523	Sea and ocean	3	3	0.200

DRINK ADRIA
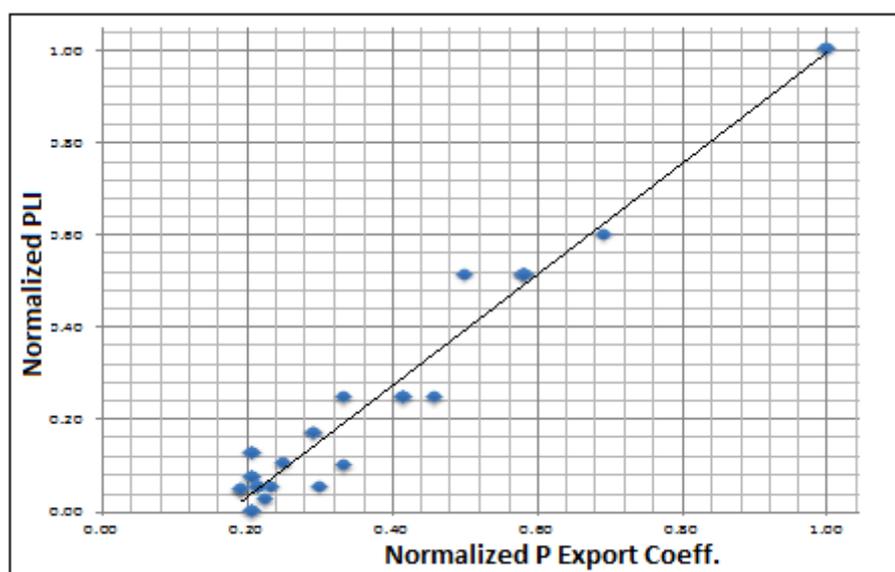
Figure 24: Relationship between Normalized Pollution Load Index (PLI) and Normalized Phosphorous export coefficients for a particular CORINE land use.

Table 7: Relationship between assigned values of land use load coefficients and literature data on phosphorous export coefficients (Wochna et al., 2011).

CLC Land use	CLC CODE	Values from different sources and expert judgment	Values from literature. all values single source	Normalized TN	Normalized TP
		TN Export Coefficient	TP Export Coefficient	Normalized TN	Normalized TP
Continuous urban fabric	111	5	1.2	0.417	0.246
Industrial or commercial units	121	6	2.5	0.500	0.512
Road and rail networks and associated land	122	5.5	1.2	0.458	0.246
Port areas	123	7	2.5	0.583	0.512
Airports	124	7	2.5	0.583	0.512
Construction sites	133	7	2.5	0.583	0.512
Green urban areas	141	3.5	0.83	0.292	0.170
Sport and leisure facilities	142	4	1.2	0.333	0.246
Non-irrigated arable land	211	12	4.88	1.000	1.000
Pastures	231	3.5	0.83	0.292	0.170
Complex cultivation patterns	242	8.3	2.33	0.692	0.477
Land principally occupied by agriculture. with significant areas of natural vegetation	243	4	0.49	0.333	0.100
Broad-leaved forest	311	3.6	0.26	0.300	0.053
Coniferous forest	312	2.5	0.36	0.208	0.074

CLC Land use	CLC CODE	Values from different sources and expert judgment	Values from literature. all values single source	Normalized TN	Normalized TP
		TN Export Coefficient	TP Export Coefficient	Normalized TN	Normalized TP
Mixed forest	313	2.8	0.26	0.233	0.053
Natural grasslands	321	2.5	0.62	0.208	0.127
Moors and heathland	322	2.7	0.13	0.225	0.027
Transitional woodland-shrub	324	2.6	0.26	0.217	0.053
Beaches, dunes, sands	331	2.5	0	0.208	-
Inland marshes	411	2.3	0.23	0.192	0.047
Peat bogs	412	2.3	0.23	0.192	0.047
Water courses	511	3	0.5	0.250	0.102

For those CORINE Land uses for which literature data is not available, expert judgment assignment of appropriate values was used. Surface water quality index (WQI_{SW}) map for the baseline year 2006 is obtained with applying of the Normalized Index of pollution Load_2006 (PLI) to CLC 2006 (level 3) map with multiplying PLI by the belonging CLC 2006 area (see Table 6) and then normalizing form 0 to 1.

Surface water quality index is assessed only for the present period (WQI_{2006}, based on CLC 2006). Surface water quality index WQI_{SW} was calculated with ArcGIS in vector format by multiplying area of particular CLC land use category with PLI value for this CLC land use category (see Table 6) and normalizing by scaling from 0 to 1.

Figure 25 presents water quality index for surface waters (WQI_{SW}), which is a potential for surface water pollution. Since WQI_{SW} is based on land use activities, these are reflecting in the water quality index. Areas with higher potential for surface water pollution (WQI_{SW}) are mostly in lowlands (i.e. Po plain in N Italy and Vojvodina in N Serbia), where there are intensive agricultural activities, industrial areas and large cities. On the contrary, areas with low surface water quality index (WQI_{SW}) are in mountainous and less populated areas (i.e. Alps, Dinarides, Apennines), where there are not many activities resulting in water pollution.

WQI_{SW} is an index, which represents potential for surface water pollution, therefore it is not necessary that in areas with high WQI actual qualitative water status is bad. Actual surface water quality can be checked from the EU member state reports, where qualitative status of surface water bodies and water resources at risk are defined for each year. In particular area surface water body status could be good, but high WQI_{SW} indicates that there is possible pollution hazard in that area because of the land use.

According to EEA (EEA 2014) and SOER reports (EEA 2015) Po valley has a very high average accumulated exceedance of the critical loads for eutrophication, which will remain also in the future, but with smaller areal extent. Almost all Adriatic area except southern BiH and part of Montenegro has a high average accumulated exceedance of the critical loads for eutrophication, but is supposed to be lower in the future. EEA studies (2012a,b) revealed that there are many water bodies with less than good ecological status; situation for chemical status is better. Total

nitrogen fertilizer application for year 2005 (kg/ha) is very high in Po valley and very high in northern Serbia and some other parts of Italy, Slovenia, Croatia and Montenegro (EEA a,b).
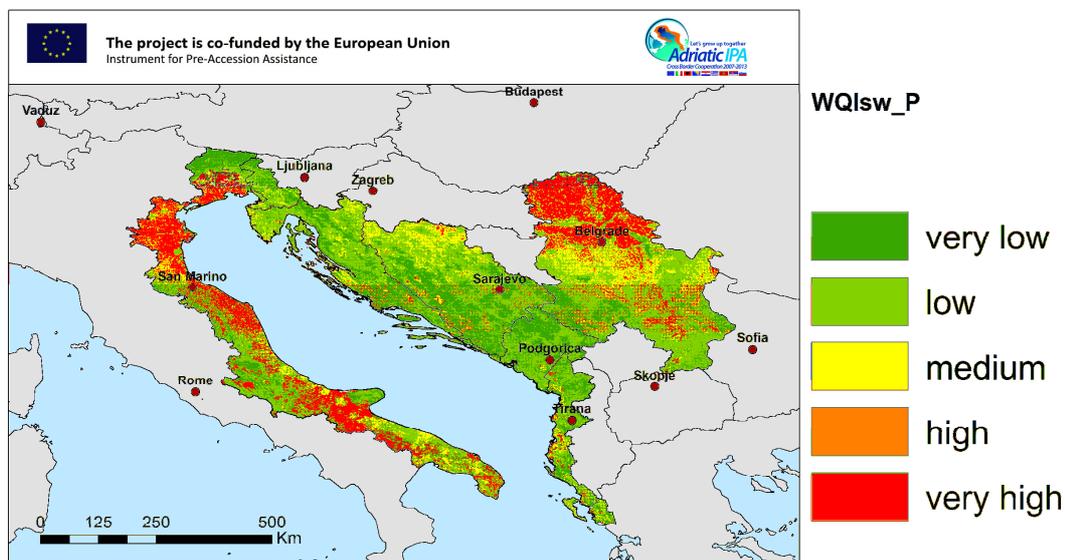

Figure 25: Potential pollution load – surface water quality index (WQIsw) for present situation

4.2.2 Groundwater quality index (WQI_{GW})

Sensitivity of groundwater bodies to pollution depends, in first place, on aquifer type or, more specifically, on their effective infiltration coefficient, which represents the part of rainfall that infiltrates into groundwater and that will eventually carry pollution load into groundwater. Groundwater quality sensitivity indicators are a function of pollution load and effective infiltration coefficient.

The basis for spatial determination of groundwater quality index is International Hydrogeological Map of Europe 1:1.500.000 - IHME1500 (Figure 26), which was made available in digital version by BGR (BGR & UNESCO 2014). HG factor is expressed as effective infiltration coefficient. High coefficient values indicate higher groundwater quality vulnerability; e.g. highly productive porous aquifers are very permeable and therefore more vulnerable to groundwater quality than areas with insignificant aquifers, which have very low permeability. For calculation of groundwater quality vulnerability HG factor as effective infiltration coefficient (Table 8) was applied to each aquifer type (Figure 27). Additionally, there are some important confined aquifers in Po plain and Friuli Venezia Giulia plain, Pannonian basin and Greece, which are lying below shallow surface porous aquifer and confining layer with low permeability. For this reason additional aquifer type was introduced: confined exstensive aquifer, for which a value of 0.2 was set (Table 8 and Figure 27).
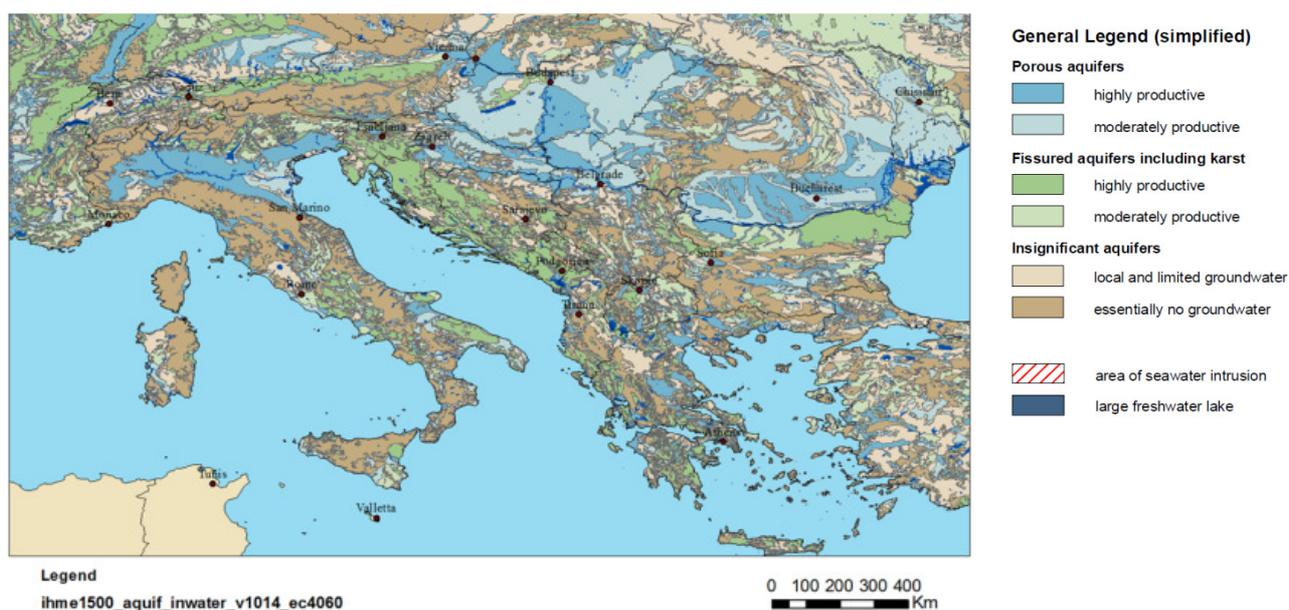
General Legend (simplified)

Porous aquifers
- highly productive
- moderately productive

Fissured aquifers including karst
- highly productive
- moderately productive

Insignificant aquifers
- local and limited groundwater
- essentially no groundwater

- area of seawater intrusion
- large freshwater lake

Legend
ihme1500_aquif_inwater_v1014_ec4060

0 100 200 300 400
Km

Figure 26: International Hydrogeological Map of Europe 1:1.500.000 (BGR & UNESCO 2014).

Table 8: HG factor - effective infiltration coefficient.

Aquifer type	Effective infiltration coefficient
1 Aquifers in which flow is mainly intergranular	
1.1 extensive and highly productive aquifers	0.6
1.2 local or discontinuous productive aquifers or extensive but only moderately productive aquifers	0.3
Confined exstensive aquifer	0.2
2 Fissured aquifers. including karst aquifers	
2.1 extensive and highly productive aquifers	0.8
2.2 local or discontinuous productive aquifers. or extensive but only moderately productive aquifers	0.4
3 Strata (granular or fissured rocks) forming insignificant aquifers with local and limited groundwater resources or strata with essentially no groundwater resources	
3.1 minor aquifers with local and limited groundwater resources	0.1
3.2 strata with essentially no groundwater resources	0.05

DRINK ADRIA
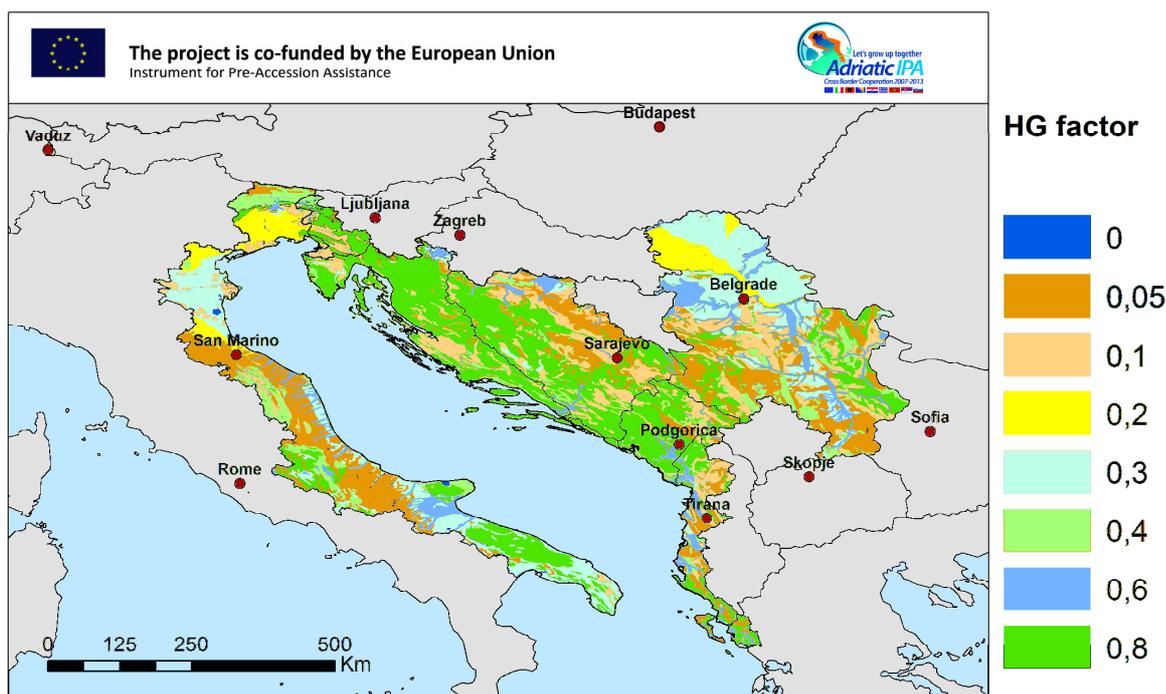
*Figure 27: Effective infiltration coefficient as HG factor.*

By multiplying surface water pollution index WQI_{SW} (Figure 25) with HG factor (table 9) in each grid we obtained groundwater pollution index (WQI_{GW}) map, which was normalized by scaling between 0 and 1.

Figure 28 presents groundwater quality index (WQI_{GW}). Since it is based on land use activities and hydrogeological characteristics, these are reflecting in the water quality sensitivity, which is rather higher only in karst region of SE Italy (in Puglia region). There are also some small areas of medium groundwater quality sensitivity (especially in E Italy and in Serbia), but most of the IPA territory shows low or very low groundwater pollution index.

WQI_{GW} is an index, which represents potential for groundwater pollution; therefore, it is not necessary that in areas with high WQI_{GW} actual qualitative water status is bad. Actual groundwater quality can be checked from the EU member state reports, where qualitative status of groundwater bodies and water resources at risk are defined for each year. In particular, area groundwater body status could be good, but high WQI_{GW} indicates that there is possible pollution hazard in that area because of the land use.

Pollution from nitrate is a major cause of poor groundwater chemical status across Europe, with agricultural sources typically having the greatest significance. The major nitrogen inputs to agricultural land are generally from inorganic mineral fertilizers and organic manure from livestock (EEA 2012a).
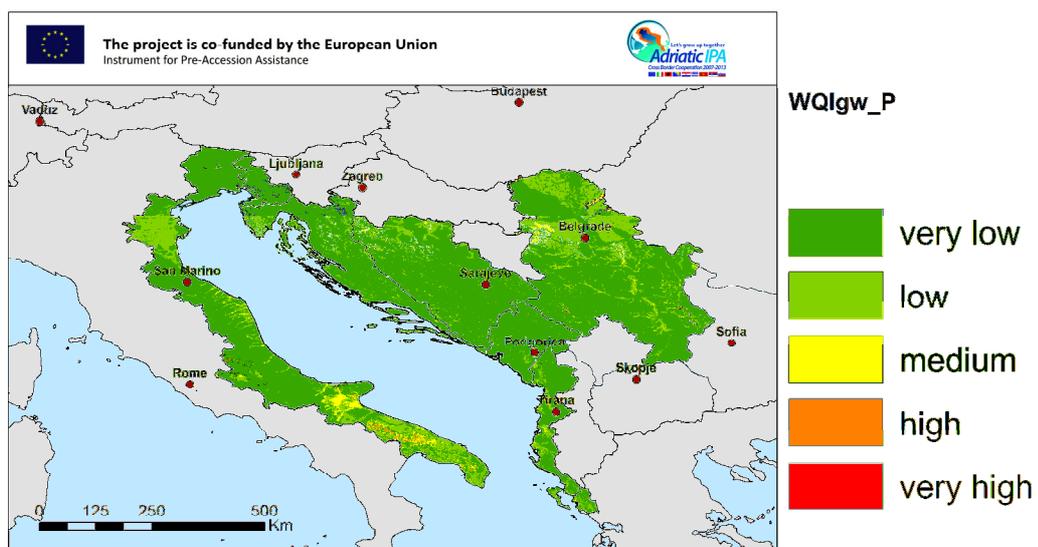
Figure 28: Potential pollution load – groundwater quality index (WQIgw) for present situation

5. ADAPTIVE CAPACITY

Adaptive capacity describes how well a system (water resources quantity and quality) can adapt or modify to cope with the climate changes. A low adaptive capacity will result in high vulnerability and vice-versa.

Adaptive capacity might reflect socio-economic and natural conditions. It may include physical, environmental and socio-economic features. In CC-WARE methodology (CC-WARE, 2014a,b) the ecosystem services index was used as natural adaptive capacity and GDP as socio economic indicator. The former expresses the role of the ecosystem in providing water in sufficient quantity and quality and the latter expresses the economic capacity of a region to compensate ecosystem service losses by technical or management measures.

## 5.1 Socio-Economic adaptive capacity

Economic status has one of the major roles in adaptation of drinking water supply to climate change and can be measured with indicator GDP (gross domestic product). Lower the GDP, lower is adaptive capacity and the system is more vulnerable to climate change impacts.

Socio-economic adaptive capacity factors are population density and economic status: GDP, employment rate etc. Population density is included already in domestic water demand, land use and potential water pollution load. Employment rate is related to GDP, therefore only GDP has been applied as socio-economic indicator. Population density was used also for downscale water demand data and GDP data from NUTS 2 to NUTS 3 scale.

The GDP data is an indicator of the output of a country or a region and was obtained from EUROSTAT database for all IPA countries except for Serbia. The GDP reflects the total value of all goods and services used for intermediate consumption in their production and it is expressed in PPS (purchasing power standards) to eliminate differences in price levels between countries. The GDP data on EUROSTAT was available on NUTS 2 level and was therefore downscaled to NUTS 3 level using population density of each NUTS 3 polygon. For Serbia GDP data was obtained from IPA partner on municipality level.

The results show GDP values are higher in western countries, such as Italy; it is high also in Montenegro (Figure 29). GDP is lower in eastern part of observed IPA territory (Slovenia, Croatia, BiH, Serbia and Albania). Moreover, there are some areas with very low GDP values in Croatia, Slovenia and Corfu which is due to low population density in these areas. This is because GDP data were downscaled to NUTS 3 by population density. The GDP map was normalized by scaling from 0 to 1 for calculation of adaptive capacity and integrated vulnerability (see chapter 6). The results show more homogeneous distribution of GDP as the result of extreme GDP values in the most developed region in Europe (Po plain area).

DRINK ADRIA
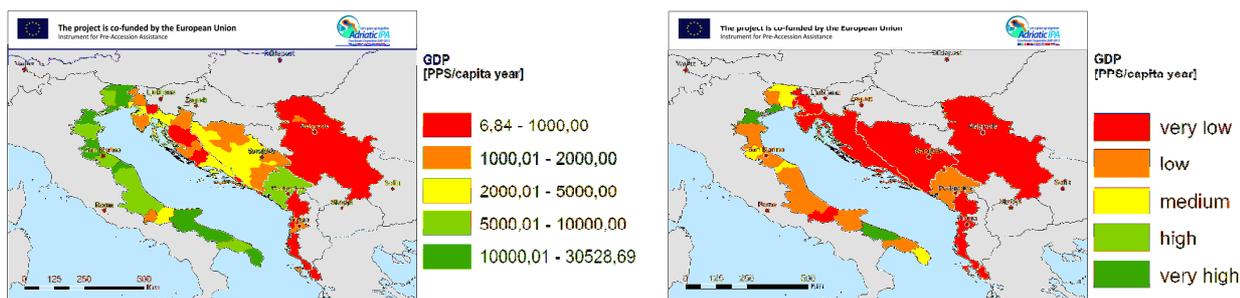
Figure 29: GDP as indicator of adaptive capacity (values and normalized map for integrated vulnerability calculation).

5.2 Natural adaptive capacity

Natural system plays an important role for drinking water sources protection. Therefore ecosystems can be natural indicator for adaptation capacity. E.g. wetlands have high protective value for drinking water protection. Ecosystem services (EES) have three functions regarding waters and water supply: Provisioning Ecosystem Service, Water Regulation and Water Quality Regulation. ESS can increase ability of a particular area to provide water supply, or a qualitative rank of potential ability of a particular area to provide excellent (both quantity and water quality) water supply, i.e. areas where ESS are more sensitive, have a higher vulnerability from water supply perspective.

For estimation of ecosystem services potential for drinking water, to each land use category and ESS type is assigned importance for water supply. With these relative weights for each land use-ESS category pair is assigned. Sum of the weights for each CLC land use class for all three ES services and their normalization create ESS value to Water Supply Index (Ecosystem Services Index ESSI) with values between 0 and 1 (CC-WARE, 2014b).

Figure 30 presents ES services in water resources perspective. Very low and low ESS index are found in valleys and plains, such as Po plain and mostly the whole E Italy and N Serbia, where all human activities are present (settlements, agriculture and industry). In contrary, low EES index occur in mountainous or less populated areas, such as, Alps, Dinarides and Apennines, which means high ES service and therefore high adaptive capacity of those areas. The results follow the fact that ES services for water supply are the highest in forested and wetland ecosystems, followed by grassland ecosystems and the lowest in agricultural ecosystems.
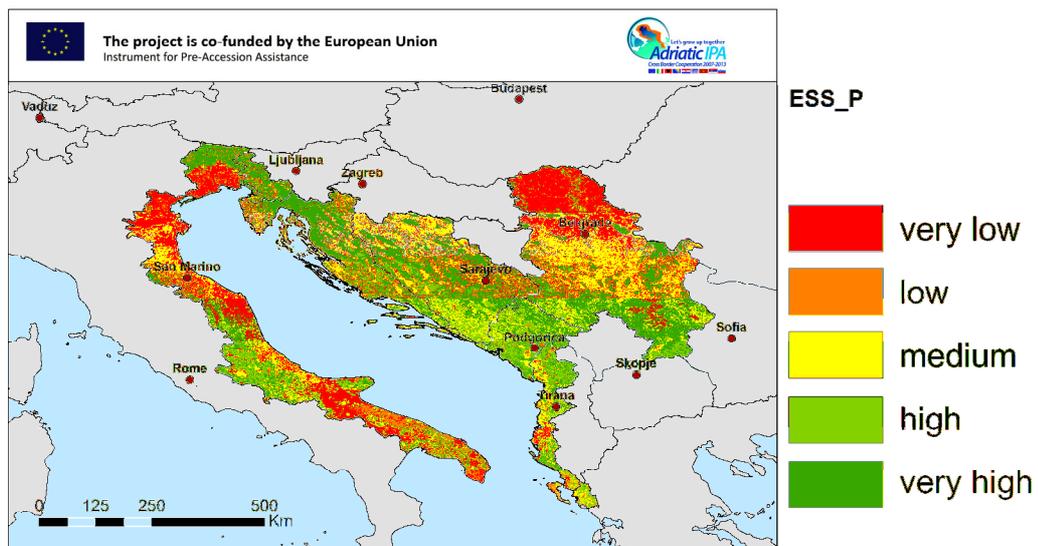
Figure 30: Ecosystem services (ESS) in water resources perspective for present situation

6. INTEGRATED ASSESSMENT OF WATER RESOURCES VULNERABILITY TO CLIMATE CHANGE

There are several methods to determine integrated (overall) vulnerability index, which is a composite of multiple quantitative indicators. The indicators are aggregated into groups according to function. According to CC-WARE methodology (CC-WARE, 2014a) two groups of indicators were selected:

- **water resources indicators group** with indicators:

      - annual local water exploitation index considering seasonality ($LWEI_{asw}$) and

      - groundwater quality index (WQI_{GW}),

and

- **adaptive capacity indicators group** with indicators:

      - GDP and

      - ecosystem services index (ESSI).

These indicators can be combined with diverse formulas or can be combined as combination of vulnerability classes to determine integrated (overall) vulnerability index.

Combining water resources indicators with adaptive capacity indicators, we get integrated vulnerability of water resources. The vulnerability is high in case of high impact, which can result from high local water exploitation index (low local total runoff, increased water demand) and high pollution potential, and low adaption capacity, such as low GDP and ESS.
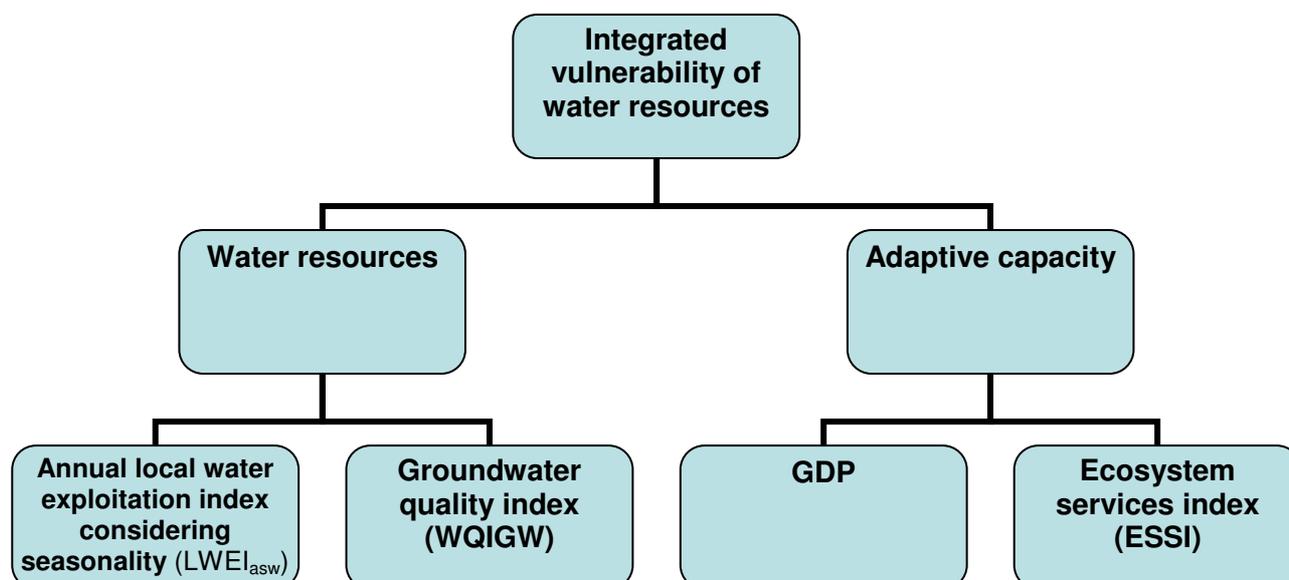

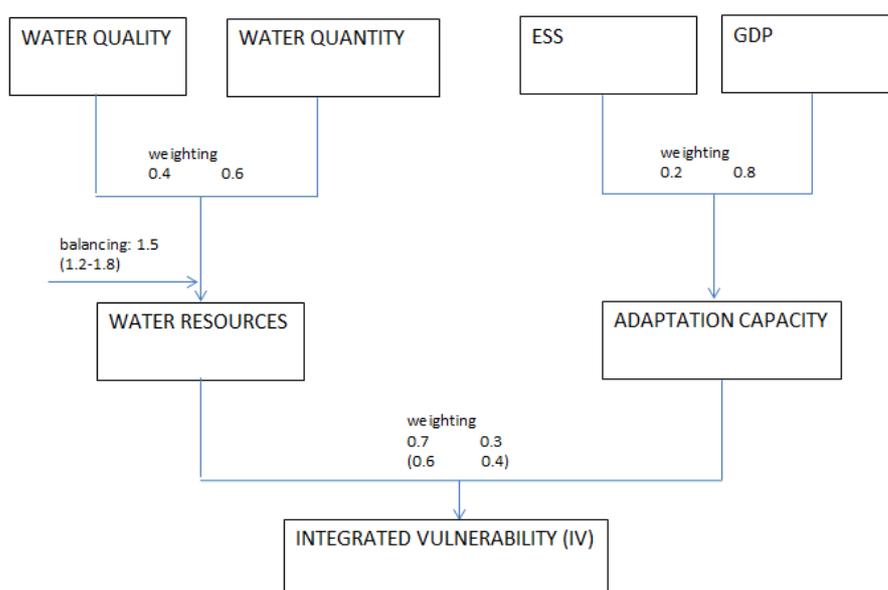*Figure 31: Determination of integrated vulnerability.*

Integrated vulnerability was calculated for present situation and for future situation considering only climate change and not land use changes.

Large groundwater systems present high groundwater availability, which is not considered in the calculation of LWEI. Large confined aqufers were added for calculation of Water qulity index for groundwater (WQI_{gw}). Therefore, such aquifers have to be considered in interpretation of integrated vulnerability.

6.1 Integrated vulnerability according to composite programming formula (HU-method)

A composite integrated vulnerability index is determined by a multi criteria method (composite programming), which provides a transparent method of assessment and organizes indicators into a hierarchical structure (Figure 31). The indicators may have various importance in forming overall vulnerability. These may be represented by assigning weights to the indicators. For comparability, these weights should be uniform over all regions, and were assessed by the CC-WARE expert group. Some indicator group may balance the indicators out, e.g. lower water quantity in a wealthy region, or low water quality in a less populated region. On the other hand, other indicators may not balance them out, e.g. enough water quantity and low water quality. The latter case indicates a "limiting factor" or "veto" situation.

Figure 32: Determination of integrated vulnerability according to composite programming.

Calculation model takes into consideration weighting and balancing factors (Figure 31). Weights represent the relative importance of each indicator within one group as viewed by the expert. Balancing factors are assigned for each group of indicators. Balancing factors reflect the relative

importance that is assigned to the maximal deviations of the indicators and limit the ability of one indicator to substitute for another. In other words, it reflects the strength of the preference for a particular objective, defining its relative importance. Generally, the balancing factors and weights are assessed by expert group.

Finally, Integrated Vulnerability Index is calculated for each group of basic indicators using the following equation:

$$IV_j = \left(\sum_{i=1}^{n_j} a_{ij} \cdot S_{ij}{}^{p_j} \right)^{1/p_j} \tag{26}$$

where
S_{ij} is the normalized value of basic indicator i in the group j of indicators,
n_j is the number of indicators in group j,
a_{ij} is the weight of expressing the relative importance of indicators in group j such that their sum equals one,
p_j is the balancing factor among indicators for group j.

Water resources and adaptive capacity are two groups in this calculation. According to balancing factors and weights from Figure 31 integrated vulnerability is then:

$$IV_{HU} = 0.7 \cdot (WR\_HU) + 0.3 \cdot (AC\_HU) \tag{27}$$

$$WR\_HU = \left(0.4 \cdot WQI_{GW}{}^{1.5} + 0.6 \cdot LWEI_{asw}{}^{1.5} \right)^{\frac{1}{1.5}} \tag{28}$$

$$AC\_HU = (0.2 \cdot (1 - ESSI) + 0.8 \cdot (1 - GDP)) \tag{29}$$

Integrated vulnerability of water resources is then:

$$IV\_HU = 0.7 \cdot \left(0.4 \cdot WQI_{GW}{}^{1.5} + 0.6 \cdot LWEI_{asw}{}^{1.5} \right)^{\frac{1}{1.5}} + 0.3 \cdot (0.2 \cdot (1 - ESSI) + 0.8 \cdot (1 - GDP)) \tag{30}$$

6.1.1 Water Resources Index (WR_HU)

The first step of determination of integrated water resources vulnerability is to consider exposure to climate change and the sensitivity of the indicators for water quantity and water quality to those changes. This step provides an understanding of the potential impacts of climate change on water resources. Water quantity indicator is $LWEI_{asw}$ and water quality indicator is WQI_{HG}. Combining these two we obtain water resources index (WRI, Figure 31). Resulting data set is normalized in order to bring proportion with other data sets for calculations.

Water resources index (Figure 32) show very low vulnerability in mountainous area of Alps and Dinarides. Conversely, very high and high water resources index is in E Italy (Puglia and Marche regions) and some parts of Po valley, on Karst region in Slovenia, in area of N BiH, N and central Serbia, parts of W Albania and in Corfu. This is due to combination of high water stress and potential pollution load.

Figure 33: Water Resources Index based on mean annual ensemble values of RegCM3, ALADIN and PROMES models for present (P) period (1991-2020).

6.1.2 Adaptive Capacity Index (AC_HU)

The second step is assessment of adaptive capacity with combining GDP and ESSI (Figure 34). Again, resulting data set is normalized in order to bring proportion with other data sets for calculations.
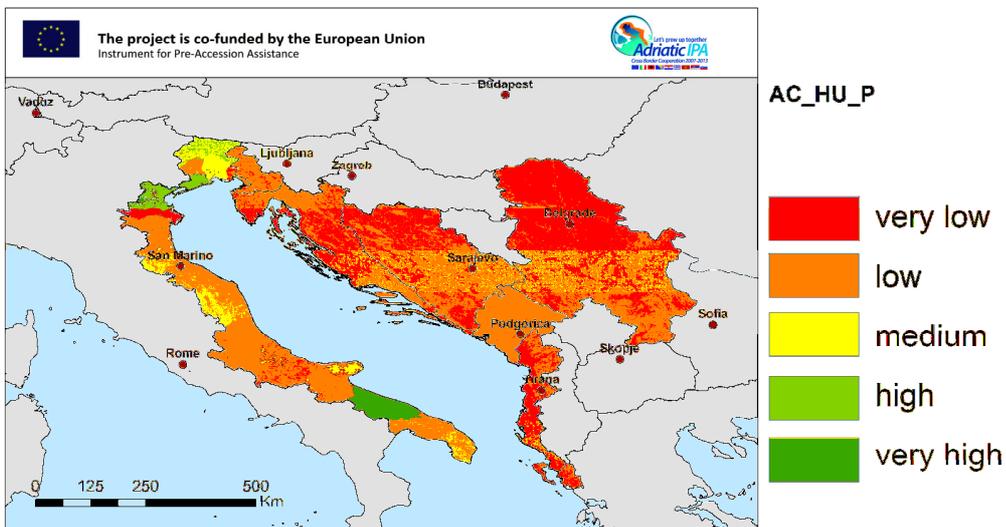
Figure 34: Adaptive capacity.

GDP (Figure 30) is dominating adaptive capacity (Figure 34), because GDP was normalized in order to bring proportion with other data sets for calculations. Consequently, the distribution in Balkan countries involved in the project is very homogeneous because of extreme GDP values in

the most developed region in Europe (Po plain area). These areas show very low and low GDP. High adaptive capacity is contrary in SE Italy (between Foggia and Bari), N part of Po plain and in Alps, in the regions with the highest GDP.

6.1.3 Integrated vulnerability (IV_HU)

Finally, integrated vulnerability index is calculated for each group of basic indicators using the equation (30).

Integrated vulnerability index in the present (Figure 35) has similar pattern as local water exploitation index (LWEI$_{asw}$, Figure 21) and water resources index (Figure 33), but the adaptive capacity lower vulnerability for one class. LWEI$_{asw}$ as indicator for water availability is dominating the integrated vulnerability, which is actually good, since also if water quality is very good, we cannot use these water resources in case there is not enough quantity.

Map of Integrated vulnerability index (Figure 35) shows low values in mountainous areas of Alps (Italy and Slovenia), Dinarides (Slovenia, N part of Croatia, Central BiH and W Serbia) and Apennines. High integrated vulnerability is in larger part of E Italy (except in SE Puglia region, W Marche region), northern, central and SE part of Serbia (except W and small scattered areas in SE), in NE and southern (coastal) BiH, major part of E Adriatic coast (from Zadar in Croatia, through BiH, Montenegro and Albania) and in Corfu.

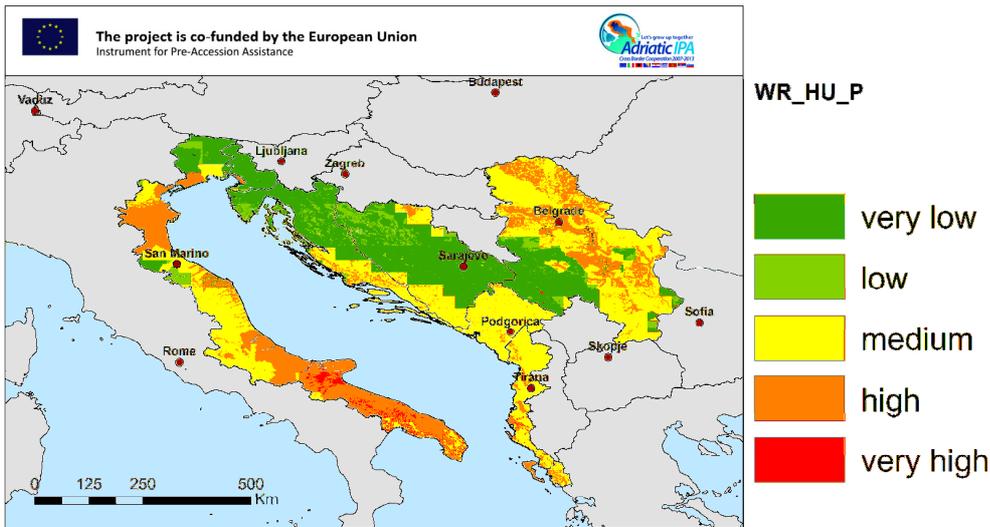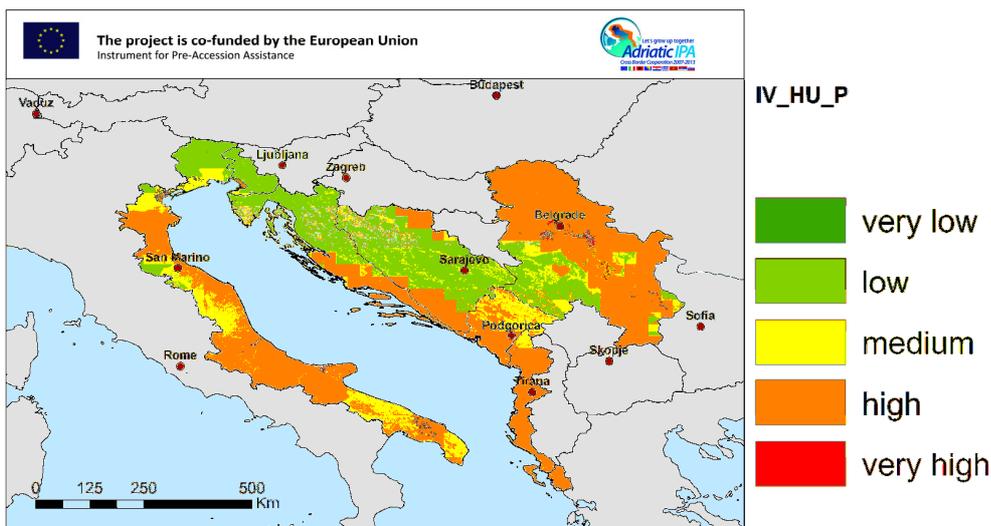*Figure 35: Integrated vulnerability index based on mean annual ensemble values of RegCM3, ALADIN and PROMES models for present (P) period (1991-2020).*

6.2 Integrated vulnerability according to expert classifying matrix (AT-method)

An integrated vulnerability index is determined according to Figure 31 by combining Water Resources Index (WR_AT) with Adaptive Capacity Index (AC_AT) with classification expert matrix.

Water quantity index (Annual local water exploitation index considering seasonality (LWEI$_{asw}$); Figure 21) and water quality index (Groundwater quality index (WQI$_{GW}$); Figure 28) are classified into five classes (very low, low, medium, high and very high). Both indices are than combined by merging on the basis of the classification matrix for obtaining the Water Resources Index as shown in Table 9.

Table 9: Water Resources Index as a function of the Annual local water exploitation index considering seasonality (LWEIasw) and Groundwater quality index (WQIGW)

Water Resources Index			Water Quantity - LWEI-annual corrected for seasonality				
			very low	low	medium	high	very high
			1	2	3	4	5
Water Quality WQI_HG	very low	A	A1	A2	A3	A4	A5
	low	B	B1	B2	B3	B4	B5
	medium	C	C1	C2	C3	C4	C5
	high	D	D1	D2	D3	D4	D5
	very high	E	E1	E2	E3	E4	E5

GDP (Figure 29) and Ecosystem services index (ESSI) (Figure 30) are classified into five classes (very low, low, medium, high and very high). Both indices are than combined by merging on the basis of the classification matrix for obtaining the Adaptive capacity Index as shown in Table 10.

Table 10: Adaptation capacity Index as a function of the GDP and Ecosystem services index (ESSI)

Adaptive Capacity			GDP per capita				
			very low	low	medium	high	very high
			1	2	3	4	5
ESSI	very low	A	A1	A2	A3	A4	A5
	low	B	B1	B2	B3	B4	B5
	medium	C	C1	C2	C3	C4	C5
	high	D	D1	D2	D3	D4	D5
	very high	E	E1	E2	E3	E4	E5

Adaptive Capacity				
very low	low	medium	high	very high

An integrated vulnerability index is determined by combining Water Resources Index (WR_AT) and Adaptive Capacity Index (AC_AT) with classification expert matrix as shown in Table 11.

Table 11: Integrated vulnerability index as a function of Water resources and Adaptive capacity index

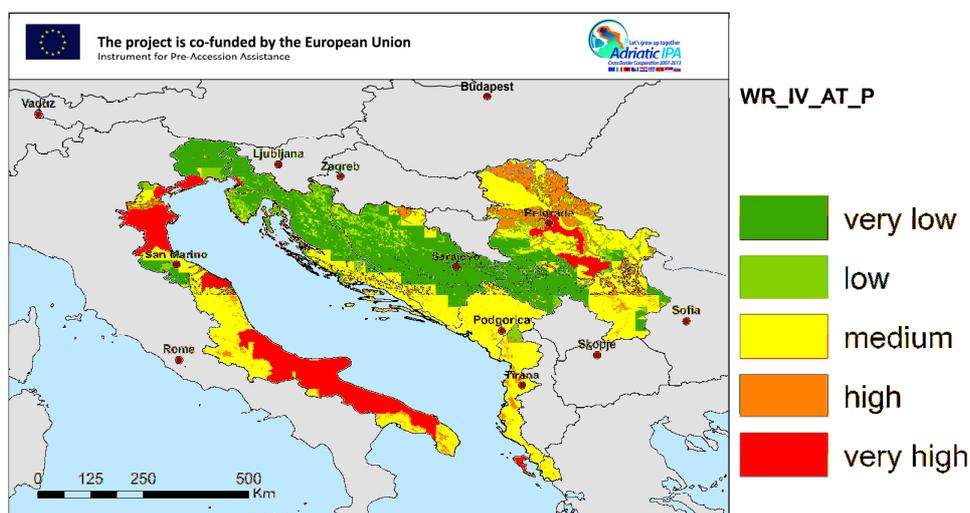|				Adaptive Capacity				
Integrated Vulnerability				very low	low	medium	high	very high
				1	2	3	4	5
Water Resources Index	very low	A		A1	A2	A3	A4	A5
	low	B		B1	B2	B3	B4	B5
	medium	C		C1	C2	C3	C4	C5
	high	D		D1	D2	D3	D4	D5
	very high	E		E1	E2	E3	E4	E5

Integrated Vulnerability				
very low	low	medium	high	very high

6.2.1 Water Resources Index (WR_AT)

The first step of determination of integrated water resources vulnerability is to consider exposure to climate change and the sensitivity of the indicators for water quantity and water quality to those changes. This step provides an understanding of the potential impacts of climate change on water resources. Combining water quantity indicator ($LWEI_{asw}$) and water quality indicator (WQI_{HG}) we obtain water resources index (WRI, Table 9).

Water resources index (Figure 36) show very low values in mountainous area of Alps and Dinarides. Conversely, very high water resources index is in Po valley and SE Italy (Puglia and Marche regions), in Karst region in Slovenia, central Serbia and in Corfu. This is due to combination of high water stress and potential pollution load.

Figure 36: Water Resources Index based on mean annual ensemble values of RegCM3, ALADIN and PROMES models for present (P) period (1991-2020).

6.2.2 Adaptive Capacity Index (AC_AT)

The second step is assessment of adaptive capacity (Figure 37) with combining GDP and ESSI (Table 10). Agricultural areas in plains have low adaptive capacity (e.g. Vojvodina, river Po plain). Mountainous areas and areas with low population density and/or high-income areas have high adaptive capacity (e.g. Alps and Apennines and Puglia region in Italy and Montenegro).
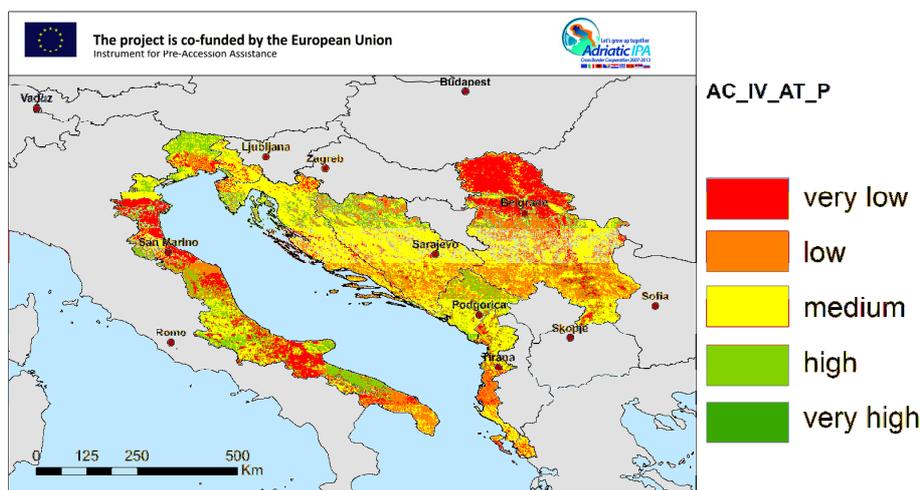

Figure 37: Adaptive capacity.

6.2.3 Integrated vulnerability (IV_AT)

Finally, integrated vulnerability index is assessed for each group of basic indicators using classification expert matrix (Table 11).

Integrated vulnerability index in the present (Figure 38) has similar pattern as local water exploitation index (LWEI$_{asw}$, Figure 21) and water resources index (Figure 32), but the adaptive capacity lower vulnerability. LWEI$_{asw}$ as indicator for water availability is dominating the integrated vulnerability, which is actually good, since also if water quality is very good, we cannot use these water resources in case there is not enough quantity.

Map of Integrated vulnerability index (Figure 38) shows low values in mountainous areas of Alps (Italy and Slovenia), Apennines (Italy) and Dinarides (Slovenia, N part of Croatia, Central BiH and W Serbia) and Apennines. High integrated vulnerability is in larger part of E Italy, northern and central part of Serbia, in NE BiH, major part of E Adriatic coast (from Zadar in Croatia, through BiH, Montenegro and Albania) and in Corfu.
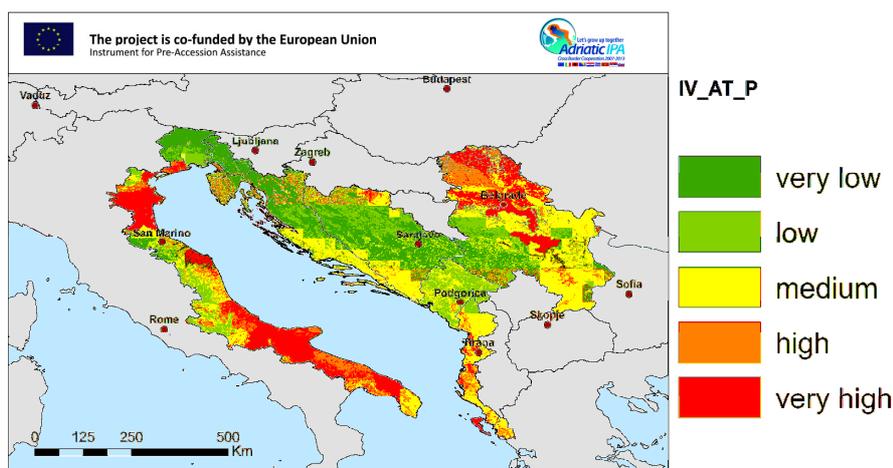
Figure 38: Integrated vulnerability index based on mean annual ensemble values of RegCM3, ALADIN and PROMES models for present (P) period (1991-2020).

6.3 Integrated vulnerability taking into account maximum values – worst case scenario (MAX-method)

Another way of determination of integrated vulnerability is combining indicators, which are normalized from 0 to 1, using maximum values. Maximum values define vulnerability, whereas mean and range can define uncertainties. This method present the worst case scenario.

6.3.1 Water Resources Index (WR_max)

Water resources index is determined as maximum value of LWEI or WQ_{gw} of each grid cell, as shown in equation 31.

$$WR\_MAX = max\ (LWEI, WQ_{GW}) \tag{31}$$

Water resources index based on maximum method (Figure 39) is very high in most of Italy, except northern Italy and SW from San Marino, in coastal part of Slovenia, southern Croatia (Dalmatia), NE and SE BiH, Montenegro, Albania, Corfu and N, central and SE part of Serbia.

Figure 39: Water Resources Index based on mean annual ensemble values of RegCM3, ALADIN and PROMES models for present (P) period (1991-2020).

6.3.2 Adaptive Capacity Index (AC_max)

Adaptive capacity is determined as maximum value of ESS or GDP of each grid cell, as shown in equation 32.

$$AC\_MAX = max\ (ESS, GDP) \tag{32}$$

Adaptive capacity based on maximum method (Figure 39) is high in mountainous and low population density areas (Alps, Dinarides, Apennines, Puglia region, most Slovenia, Croatia, BiH, Montenegro, E Albania, southern Serbia) and areas with high GDP (e.g. N Po valley in Veneto region). Very low adaptive capacity is in northern Serbia due to large agricultural areas- Low adaptive capacity is in S Po valley, coastal area of Italy (except Puglia) and coastal areas of Albania.
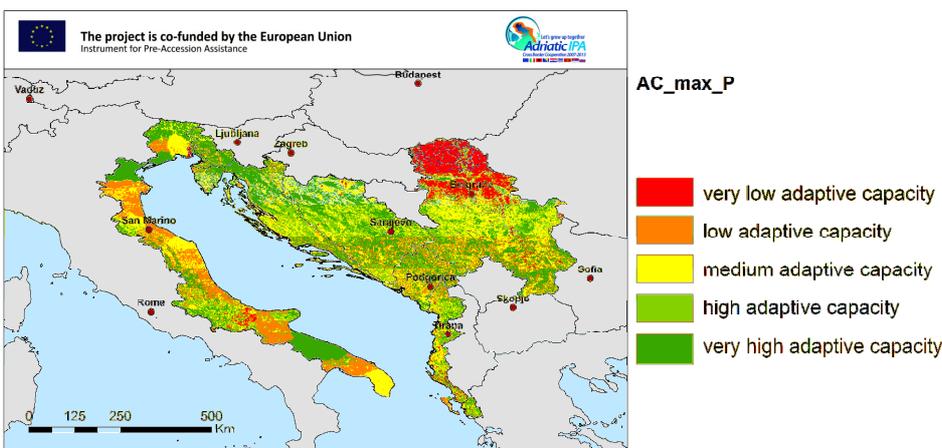
Figure 40: Adaptive capacity.

6.3.3 Integrated vulnerability (IV_max)

Integrated vulnerability is determined as maximum value of Water resources index or Adaptive capacity of each grid cell, as shown in equation 33.

$$IV\_MAX = max (WR, AC) \tag{33}$$

According to maximum method, presenting worst case scenario, a major part of IPA Adriatic area has very high integrated vulnerability in the most of Italy, except northern part (Friuli Venezia Gulia region and N Veneto region) and NW from San Marino, where integrated vulnerability is low to medium. Very high integrated vulnerability is in coastal part of Slovenia, southern Croatia (Dalmatia), NE and SE BiH, Montenegro, Albania, Corfu and northern, central and SE Serbia. Low integrated vulnerability is in mount nous regions (Alps and Dinarides).
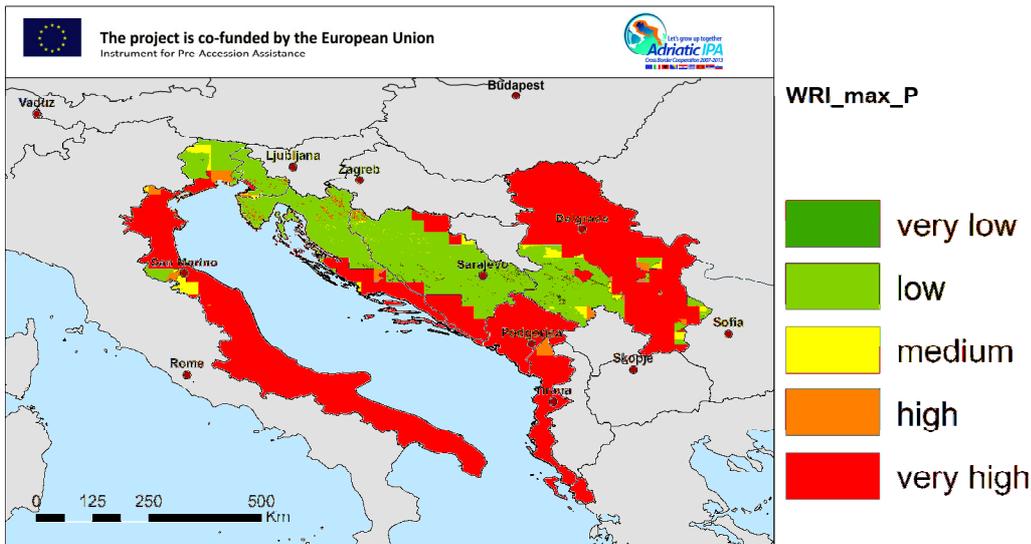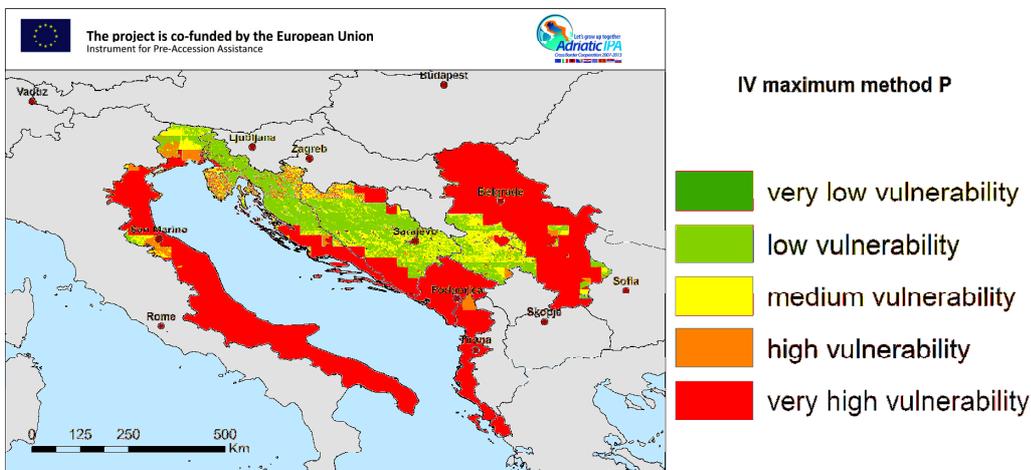

Figure 41: Integrated vulnerability index based on mean annual ensemble values of RegCM3, ALADIN and PROMES models for present (P) period (1991-2020).

7. SUMMARY

Vulnerability of freshwater resources as potential drinking water resources is characterised by several indicators, describing water availability and increasing demand and the future qualitative state of the system compared to drinking water standards. 'Vulnerability is a function of the character, magnitude and rate of climate variation to which a system is exposed, its sensitivity and its adaptive capacity' (IPCC, 2007). The methodology applied in the DRINKADRIA project builds on this description of vulnerability by examining the exposure (predicted changes in the climate), sensitivity (the responsiveness of a system to climatic influences) and adaptive capacity (the ability of a system to adjust to climate change) of a range of indicators. Exposure is the change expected in the climate for a range of variables including temperature and precipitation. Sensitivity is the degree to which systems respond to the changes. For example less precipitation may reflect in substantial reduction of water availability in a small river basin or aquifer. The ecosystem services and GDP were applied as adaptive capacity indicators. Integrated water resources vulnerability is an overall indicator characterized by set of indicators referring to water quantity, water quality and adaptive capacity.

The climate is the main natural driver of the variability in the water resources. Atmospheric precipitation, air temperature and evapotranspiration are commonly used for assessing and forecasting the water availability and were derived from three RCMs (RegCM3, ALADIN-Climate and PROMES), which are based on A1B SRES IPCC scenario and bias corrected based on daily observations extracted from the E-OBS data base. Spatial resolution is 25-km. Studied time periods were 1961-1990 (baseline climate), 1991-2020 (present climate) and 2021-2050 (future climate).

Temperature. According to the comparison of future and present mean temperatures found by selected models suggest increase of temperature in individual regions in all seasons. The highest and also most extensive temperature increase occur during the summer in S Serbia, Central and SE Montenegro, E and S Albania, Corfu and partly in SE Italy. The highest temperature increase in spring are in small area of N Albania, in fall in NE Italy, northern part of Serbia and on southern Croatian Islands, while in winter the highest increase occur in Slovenian part of Alps and Dinarides, northern Dinarides in Croatia and E Italy (eastern Po Vally). Generally, the highest changes in temperatures are shown in summer and winter, while in spring the trend of changes are significally lower. Among regions the highest increasing trend is present in central Balkan Peninsula (Serbia, BIH, Montenegro, Albania) in all seasons, with a small difference in winter where the highest increases occur in S Alps and N part of Dinarides, resulting less snow in the future and consequently less water reserves in rivers for spring and summer periods. Temperature values are for most of the partner countries in adequate range regarding observed data and are acceptable for water balance calculations.

Precipitation. Distribution of precipitation in all periods generally follow the geomorphological characteristics of the area and a decreasing trend is observed in the future. The highest precipitation is observed in Alps, Dinarides and Apenines, but in Dinarides (in BIH) in the future a significant decreasing trend in rainfall is observed. In Central Balkan, S Albania, Corfu and central part of E Italy (E Emiglia Romagna and Marche regions) lower precipitation occur (yellow), while the lowest precipitation is in southern half of E Italy (Abruzzo, Molise and Puglia regions) and the entire eastern half of Serbia, but in Serbia rather increasing precipitation trend is observed in the future. For most countries the pattern of modelled precipitation is in compliance with measured data. In this point it has to be stressed that this is a regional analysis with the coarse spatial resolution (25 km grid), based on E-OBS data base, which has deficiency in underestimated

values in mountainous areas, which is the case in the Alps (north-eastern Italy and north-western Slovenia), Apennines (central Italy) and Dinarides (Croatia, BiH, south-west Serbia). Besides, local spatial heterogeneities are however not captured by the coarse spatial resolution. Precipitation is also underestimated in eastern central Serbia and Gargano peninsula in Italy.

The changes in precipitation between the present (1991-2020) and base (1961-1990) period and between the future (2021-2050) and present (1991-2020) period show generally positive trends (increasing of precipitation) both for the present in relation to the base as well as for the future in relation to the present. Significal decreasing of precipitation trends are noticeable only in individual parts of the eastern Italy (Puglia region).

Actual evapotranspiration. High annual AET for all periods is observed in mid-northern and south Italy, in W Slovenia, most part of Croatia, along the whole eastern Adriatic coast (Croatia, BiH, Montenegro, Albania and Corfu), northern BiH and in the future also in central Serbia. The increasing trend in the future can be observed and is the most significant in BiH and central Serbia. Low AET occur for all periods in mid-eastern Italy (Puglia region – Gargano Promotory), eastrn part of Montenegro and N and S Serbia. AET is calculated indirect with use of PET, which is underestimated in lowland areas, consequently, AET is lower than national modelled AET values in many lowland areas of the study area. In some cases AET is higher (e.g. Alps, Dinarides) than national modelled values. Due to the coarse spatial resolution (25 km grid) local spatial heterogeneities are however not captured, which is the case of north-eastern Italy, where modelled AET on smaller scale are very scattered, but within the range, except for mountainous area. The AET pattern will be preserved in the future, but general increasing in the absolute values are estimated in the future.

Relative differences in precipitation between the present (1991-2020) and base (1961-1990) period show relative increasing of annual AET in mid-northern Italy (up to 6 %), W Slovenia, northern half of Croatia, most of BiH and Montenegro, central Albania and large part of Serbia without the north and partly south-east. Relative differneces between the future (2021-2050) and present (1991-2020) period show similar increasing and even more significant pattern of changes. The AET will be even more higher which is especially seen in Serbia and the central part of Balkan Peninsula. The only decrease of AET are observed for both estimated comparison in mid-eastern Italy (Puglia region – Gargano Promotory).

Water quantity. Water exploitation index (WEI) or water stress is the ratio of total water demand (domestic, industrial and agricultural) to the available amount of renewable water resources that consists of surface water and groundwater safe yield (river discharge or runoff and groundwater recharge).

Local total runoff is available amount of renewable water resources. In all periods total runoff is high in the Alps, northern Dinarides and around Skadar lake (border between Montenegro and Albania), whereas in all other parts it is significantly lower, which means very low annual recharge in those areas. The lowest total runoff is in SW part of Italy (especially Puglia region – Gargano Promotory) and N Serbia. LTR is calculated with as difference between precipitation and AET. Precipitation is underestimated in mountainous areas, whereas AET is underestimated in lowland areas and overestimated in mountainous areas. Consequently, runoff is underestimated in some mountainous areas (Alps, Dinarides, Apennines) and overestimated in some plain areas. LTR is underestimated also in eastern-central Serbia. Due to the coarse spatial resolution (25 km grid) local spatial heterogeneities are however not captured.

DRINK ADRIA

Relative changes of LTR between present (1991-2020) and base (1961-1990) show higher LTR (mean more recharge; up to 16 %) N Italy, W Slovenia and Istra Peninsula (Croatia). Lower LTR is observed in central Balkan Peninsula (northern Croatia, SE half of BiH and Montenegro and E Serbia, while for E half of Serbia, W Balkan Peninsula (S and coastal Croatia, W BiH and Montenegro, Albania and Corfu scenarios show the reduction of local total runoff up to 20 %. Relative changes of LTR between future (2021-2050) and present (1991-2020) period show that higher LTR in the future would be only in some parts of central Serbia. Conversely, lower LTR (up to 30 %) will be in some parts of SE half of Italy and W Balkan Peninsula (S half of Croatia, SW BiH, W Montenegro, Albania and Corfu). Scenarios for all other areas show smaller reduction of local total runoff.

Generally, scenarios show that there would be up to 30 % less recharge and water available in the future in southern Italy and Greece and around 20 % less recharge in southern Croatia (Dalmatia), southern Serbia and coastal part of Montenegro, whereas in other areas there is no significant change in LTR. Considering 10-20% uncertainty, all other parts of the region are inside this range. Nevertheless, also small regional changes can influence local water supply.

Map of changes in average annual water availability under the LREM-E scenario by 2030 (EEA 2005) shows diminishing of water availability from 5-25 % in southern Italy and Greece. There is no data for Croatia, Serbia, Montenegro and Albania.

Total water demand (WD) was evaluated as the sum of domestic (DWD), agricultural (AGRWD) and industrial (INDWD) water demand. For future water demand four scenarios of water demand changes have been applied: 10 % decrease, no change and 10 % and 25 % increase of WD. The pattern of DWD is following the population density. Higher domestic water demand is attached to the plains (i.e. Po plain) and the territories of major cities. Conversely, lower domestic water demand is found in mountainous and less accessible regions. AGRWD is very high in Corfu and Albania because of irrigation. In Serbia pattern is very scattered due to the data scale on Municipality level. All other countries show very low AGRWD. INDWD is high in the Po plain and the most southern parts of Italy, in Slovenia (especially the coastal area) and central Serbia. High industrial water demand in Montenegro is due to hydropower plant water demand, which could not be subtracted from the data, therefore this has to be considered in all other results. WD (total water demand) is higher in Po plain and SE part in Italy, W Slovenia (especially in coastal area), central Serbia, in Montenegro Albania and Corfu. While high WD in Italy, Slovenia, Serbia and Montenegro is the result of higher industrial water demand, in Albania and Corfu is of higher agricultural and domestic water demand. Due to the selection of future scenarios, the pattern for all maps is practically the same.

Annual water exploitation index, considering seasonality (LWEI$_{asw}$) – **water stress** is high or very high in the whole E Italy, except in small part of Apennines and the Alps, on Karst Plateau in Slovenia, in SW Croatia, SW and partly N of BiH, a large part of Serbia, except the west, in Montenegro, Albania and Corfu. Very low water stress occurs in Alps and Dinarides, part of Apennines (W of San Marino) and western Serbia. There are only few small areas of medium water stress: parts of Po plain, in central Croatia, N Albania and individual parts of Serbia. In the future, the pattern will be the same with small changes, there are some more areas with very high stress.

The applied methodology for determination of water stress was based on estimation of the water balance for single grid cell (25 km), in which river inflow is not considered. In most of the areas with high water stress, rivers are already used for irrigation or other purposes, but one has to be aware that rivers are also limited resource. Due to large scale of the study, results have to be considered

DRINK ADRIA

with due reservation and as indicator. The resulting maps are actually indicators for measures to be applied in a region with high water stress. In some cases, measures have already been applied. For example, in Serbia Belgrade does not have problems with water quantity due to Sava riverbank filtration; whereas some other regions in Serbia have already problems with water quantity and will have greater in the future. Another example is Trieste province in Italy, which has medium water stress and high water stress in the Trieste city area due to very high population density, but in reality the water stress is lower due to water storage in large porous aquifer of Soča/Isonzo Low Plain, which is used for water supply. This is the case also for Po Plain in Italy, which has high water stress, but the actual quantity status is good due to the large volume of water stored in large confined porous aquifer in the Po plain and in the plain of the Friuli Venezia Giulia Region. These porous aquifers make the area resilient to large exploitation. Nevertheless, the LWEI map highlights critical exploitation indexes in the alluvial fans located at transition area between NE Apennines and the Po river plain. This is consistent with an observed bad water quantity status in some of these aquifers that is mainly due to past and present overexploitation.

EEA (2015) study is showing high water stress in southern Italy for present and future. For northeastern Italy and Slovenia there is low water stress for present and future. Most of other parts of Italy there is medium water stress. There is no data for Croatia, Serbia, Montenegro and Albania. Similarly, Flörke et al. (2011) show severe water stress (more than 0,4) for present state in central and south Italy and north-east Greece. They used different future scenarios for projection to 2050 (Economy First Scenario and Sustainability Eventually Scenario). The first one shows sever water stress in the most part of Italy, south-east Serbia, central Albania and eastern Greece, whereas the second one is milder and show only some areas with severe stress in Italy and Greece (Flörke et al. 2011, EEA 2012c). Differences are due to different scenarios and lower resolution (simulations based on river basin).

Water quality. Main driver for water quality vulnerability is land use; therefore land use load coefficients were applied as water quality indicator – water quality index (WQI). Water quality index is sensitivity of water body to pollution and represents potential for water pollution. Therefore it is not necessary that in areas with high WQI actual qualitative water status is bad. In particular area water body status could be good, but high WQI indicates that there is possible pollution hazard in that area because of the land use.

Surface water quality - water quality index for surface waters (WQI$_{SW}$) is based on land use activities, which are reflecting in the water quality index. Areas with higher potential for surface water pollution are mostly in lowlands (i.e. Po plain in N Italy and Vojvodina in N Serbia), where there are intensive agricultural activities, industrial areas and large cities. On the contrary, areas with low surface water quality index are in mountainous and less populated areas (i.e. Alps, Dinarides, Apennines), where there are not many activities resulting in water pollution.

According to EEA (EEA 2014) and SOER reports (EEA 2015) Po valley has a very high average accumulated exceedance of the critical loads for eutrophication, which will remain also in the future, but with smaller areal extent. Almost all Adriatic area except southern BiH and part of Montenegro has a high average accumulated exceedance of the critical loads for eutrophication, but is supposed to be lower in the future. EEA studies (2012a,b) revealed that there are many water bodies with less than good ecological status; situation for chemical status is better. Total nitrogen fertilizer application for year 2005 (kg/ha) is very high in Po valley and very high in northern Serbia and some other parts of Italy, Slovenia, Croatia and Montenegro (EEA a,b).

Groundwater quality index (WQI$_{GW}$). Sensitivity of groundwater bodies to pollution depends on aquifer type or, more specifically, on their effective infiltration coefficient, which represents the part

of rainfall that infiltrates into groundwater and that will eventually carry pollution load into groundwater. Therefore groundwater quality sensitivity indicators are a function of pollution load and effective infiltration coefficient and are reflecting in the water quality sensitivity. Groundwater quality index is rather higher only in karst region of SE Italy (in Puglia region). There are also some small areas of medium groundwater quality sensitivity (especially in E Italy and in Serbia), but most of the IPA territory shows low or very low groundwater pollution index. There are large karst areas in IPA ADRIATIC area (Alps, Dinaric karst, central and southern Italy) with low pollution index, because general land use are forests and grasslands, but it has to be noted that these areas are vulnerable to pollution, because of rapid infiltration. Therefore, in local scale the pollution load can be much higher due to land uses, which cause more pollution load, such as urbanization, roads, agriculture, etc.

Pollution from nitrate is a major cause of poor groundwater chemical status across Europe, with agricultural sources typically having the greatest significance. The major nitrogen inputs to agricultural land are generally from inorganic mineral fertilizers and organic manure from livestock (EEA 2012a).

Adaptive capacity describes how well a system (water resources quantity and quality) can adapt or modify to cope with the climate changes. A low adaptive capacity will result in high vulnerability and vice-versa. Adaptive capacity might reflect socio-economic and natural conditions. Socio-economic adaptive capacity factors are population density and economic status: GDP, employment rate etc. Population density is included already in domestic water demand, land use and potential water pollution load; therefore only GDP was applied. Natural system plays an important role for drinking water sources protection; therefore ecosystems can be natural indicator for adaptation capacity

GDP expresses the economic capacity of a region to compensate water stress by technical or management measures. GDP values are higher in western countries, such as Italy; it is high also in Montenegro. GDP is lower in eastern part of observed IPA territory (Slovenia, Croatia, BiH, Serbia and Albania). Moreover, there are some areas with very low GDP values in Croatia, Slovenia and Corfu which is due to low population density in these areas. This is because GDP data were downscaled to NUTS 3 by population density.

Ecosystem services express the role of the ecosystem in providing water in sufficient quantity and quality. Very low and low ESS index are found in valleys and plains, such as Po plain and mostly the whole E Italy and N Serbia, where all human activities are present (settlements, agriculture and industry). In contrary, low EES index occur in mountainous or less populated areas, such as, Alps, Dinarides and Apennines, which means high ES service and therefore high adaptive capacity of those areas. The results follow the fact that ES services for water supply are the highest in forested and wetland ecosystems, followed by grassland ecosystems and the lowest in agricultural ecosystems.

Integrated vulnerability index is a composite of multiple indicators, which are aggregated into groups according to function: **water resources indicators group** with annual local water exploitation index considering seasonality ($LWEI_{asw}$) and groundwater quality index (WQI_{GW}), and **adaptive capacity indicators group** with GDP and ecosystem services index (ESSI).

Water resources index show very low vulnerability in mountainous area of Alps and Dinarides. Conversely, very high and high water resources index is in SE Italy (Puglia and Marche regions) and some parts of Po valley, in Karst region in Slovenia, northern BiH, northern and central Serbia,

parts of W Albania and in Corfu. This is due to combination of high water stress and potential pollution load.

Adaptive capacity. GDP is dominating adaptive capacity, because GDP was normalized in order to bring proportion with other data sets for calculations. Consequently, the distribution in Balkan countries involved in the project is very homogeneous because of extreme GDP values in the most developed region in Europe (Po plain area). These areas show very low and low GDP. High adaptive capacity is in contrary in SE Italy (between Foggia and Bari), N part of Po plain and in Alps, in the regions with the highest GDP. Agricultural areas in plains have low adaptive capacity (e.g. Vojvodina, river Po plain). Mountainous areas and areas with low population density and/or high-income areas have high adaptive capacity (e.g. Alps and Apennines and Puglia region in Italy and Montenegro).

Integrated vulnerability index has similar pattern as local water exploitation index and water resources index, but the adaptive capacity lower vulnerability for one class. $LWEI_{asw}$ as indicator for water availability is dominating the integrated vulnerability, which is actually good, since also if water quality is very good, we cannot use these water resources in case there is not enough quantity. Integrated vulnerability index is low in mountainous areas of Alps (Italy and Slovenia), Dinarides (Slovenia, N part of Croatia, Central BiH and W Serbia) and Apennines. High integrated vulnerability is in larger part of E Italy (except in SE Puglia region, W Marche region), northern, central and SE part of Serbia (except W and small scattered areas in SE), in NE and southern (coastal) BiH, major part of E Adriatic coast (from Zadar in Croatia, through BiH, Montenegro and Albania) and in Corfu.

Conclusion

Taking into consideration the degree of generalization (25 km grid), the large scale territory of investigation (whole IPA Adriaric region) and the used information, the resulting assessment of the integrated vulnerability on the transnational level gives a generalized representation on the main trends and impacts of the different driving forces. For this, in further investigations from the water supply point of view, additional system of indices has to be applied in more detailed scale, estimating the water supply system performance such as water shortage index, reliability in time (by years, months), reliability by volume, etc.

8. REFERENCES

Baltas E. (2007) Spatial distribution of climatic indices in northern Greece. Meteorol. Appl. 14: 69-78.http://onlinelibrary.wiley.com/doi/10.1002/met.7/pdf

Beguería S. Vicente-Serrano SM (2007) Package ‚SPEI' - Calculation of the Standardised Precipitation-Evapotranspiration Index. Program instructions. 16p.
http://cran.r-project.org/web/packages/SPEI/SPEI.pdf

Budyko MI (1974) Climate and life. Translated from Russian. by D. H. Miller. Academic Press. Orlando. FL. 508 pp.

Busuioc A. Dumitrescu A. Baciu M. Cazacioc L. Cheval S (2010) RCM performance in reproducing temperature and precipitation regime in Romania. Application for Banat Plain and Oltenia Plain. Romanian J Meteor. 10(2): 1-19.

Castro M. Fernandez C. Gaertner MA (1993) Description of a mesoscale atmospheric numerical model. In Diaz JI. Lions JL (eds) Mathematics. climate and environment. Rech. Math. Appl. Ser.. vol. 27. Ser. Masson: Paris: 230–253.

CC-WARE (2014a) CC-WARE Mitigating Vulnerability of Water Resources under Climate Change, report WP3: Vulnerability of Water Resources in SEE. 84pp., Available at: *http://www.ccware.eu/output-documentation/2-uncategorised/23-output-wp3.html*

CC-WARE (2014b) CC-WARE Mitigating Vulnerability of Water Resources under Climate Change, report WP4: Criteria and indicator-based assessment of ecosystem services (ES) in SEE, pp.51., Available at:
http://www.ccware.eu/output-documentation/2-uncategorised/24-output-wp4.html

CC-WaterS (2010) Climate change and impacts on water supply, CC-WaterS monograph. December 2010. 238 pp., Available at: *http://www.ccware.eu/output-documentation/2-uncategorised/23-output-wp3.html*

Déqué M (2007) Frequency of precipitation and temperature extremes over France in an anthropogenic scenario: Model results and statistical correction according to observed values. Global and Planetary Change 57: 16–26.

Dingman SL (1992) Physical Hydrology. Prentice Hall. Upper Savage. New Jersey. 646 pp.

Doerr A. H. (1963) De Martonne's Index of Aridity and Oklahoma's Climate, in: Proceedings of the Oklahoma Academy of Science, Vol. 43, University of Oklahoma, p. 211-213.

EC DG Environment (2010) Background Document on Vulnerability Indicators for the project Climate Adaptation – modelling water scenarios and sectoral impacts. Contract N° DG ENV.D.2/SER/2009/0034

EEA (2005) European environment outlook. EEA Technical report No 4/2005, European Environment Agency, Copenhagen, Denmark. 87 pp.

EEA (2007) Land-use scenarios for Europe: qualitative and quantitative analysis on a European scale. EEA Technical report No 9/2007.76pp.

EEA (2012a) European waters — assessment of status and pressures. EEA Technical report No 8/2012, European Environment Agency, Copenhagen, Denmark. 96 pp., doi:10.2800/63266

EEA (2012b) European waters — current status and future challenges, Synthesis. EEA Technical report No 9/2012, European Environment Agency, Copenhagen, Denmark. 52 pp., doi:10.2800/63931

EEA (2012c) Water resources in Europe in the context of vulnerability; EEA 2012 state of water assessment. EEA Report No 11/2012.

EEA (2014) Effects of air pollution on European ecosystems. Past and future exposure of European freshwater and terrestrial habitats to acidifying and eutrophying air pollutants, EEA Technical report No 11/2014, European Environment Agency, Copenhagen, Denmark.

EEA (2015) The European environment — state and outlook 2015: synthesis report, European Environment Agency, Copenhagen. 205pp., doi:10.2800/944899

Elguindi N. Bi X. Giorgi F. Nagarajan B. Pal J. Solmon F. Rauscher S. Zakey A (2007) RegCM Version 3.1 User's Guide. Trieste: PWCG Abdus Salam ICTP. 57 pp.

Farda A. Déqué M. Somot S. Horányi A. Spiridonov V. Tóth H (2010) Model Aladin as Regional Climate Model for Central and Eastern Europe. Stud Geophys AS CR: 313-332.

Flörke, M., Wimmer, F., Laaser, C., Vidaurre, R., Tröltzsch, J., Dworak, T., Marinova, N., Jaspers, F., Ludwig, F., Swart, R., Giupponi, C., Bosello, F., Mysiak J. (2011) Climate Adaptation – modelling water scenarios and sectoral impacts. Final Report. Center for Environmental Systems Research (CERS) in cooperation with Ecologic, Alterra and CMCC. 157 pp. Available at: http://climwatadapt.eu/sites/default/files/ClimWatAdapt_final_report.pdf /assessed 30 May 2016/

Formayer H. Haas P (2010) Correction of RegCM3 model output data using a rank matching approach applied on various meteorological parameters. In Deliverable D3.2 RCM output localization method (BOKU-contribution of the FP 6 CECILIA project on http://www.cecilia-eu.org/).

FOOTPRINT (2006) Characteristics of European groundwater vulnerability scenarios. DL10. 6FP programe. Project no. 022704 (SSP).

Gaertner MA. Dominguez M. Garvert M (2010) A modelling case-study of soil moisture–atmosphere coupling. Quarterly Journal of the Royal Meteorological Society 136(S1): 483-495. DOI: 10.1002/qj.541.

Gain AK. Giupponi C. Renaud FG (2012) Climate Change Adaptation and Vulnerability Assessment of Water Resources Systems in Developing Countries: A Generalized Framework and a Feasibility Study in Bangladesh. Water . 4. 345-366.

Gerrits AMJ. Savenije HHG. Veling EJM. Pfister L (2009) Analytical derivation of the Budyko curve based on rainfall characteristics and a simple evaporation model. Water Res. Research 45. W04403. doi:10.1029/2008WR007308.

Haylock MR. Hofstra N. Klein Tank AMG. Klok EJ. Jones PD. New M (2008) A European daily high-resolution gridded data set of surface temperature and precipitation for 1950-2006. J Geophys Res. 113. D20119. doi:10.1029/2008JD010201.

Hewitt CD (2004) Ensembles-based predictions of climate changes and their impacts. Eos. Transactions American Geophysical Union 85(52): 566. doi: 10.1029/2004EO520005.

IPCC TAR WG1 (2001) Climate Change 2001: The Scientific Basis. Contribution of Working Group I to the Third Assessment Report of the Intergovernmental Panel on Climate Change. Houghton JT. Ding Y. Griggs DJ. Noguer M. van der Linden PJ. Dai X. Maskell K. Johnson CA. (eds.) Cambridge University Press.

DRINK ADRIA

IPCC, 2014a: Climate Change 2014: Impacts, Adaptation, and Vulnerability. Part A: Global and Sectoral Aspects. Contribution of Working Group II to the Fifth Assessment Report of the Intergovernmental Panel on Climate Change [Field, C.B., V.R. Barros, D.J. Dokken, K.J. Mach, M.D. Mastrandrea, T.E. Bilir, M. Chatterjee, K.L. Ebi, Y.O. Estrada, R.C. Genova, B. Girma, E.S. Kissel, A.N. Levy, S. MacCracken, P.R. Mastrandrea, and L.L.White (eds.)]. Cambridge University Press, Cambridge, United Kingdom and New York, NY, USA, 1132 pp. Available at: http://www.ipcc.ch/report/ar5/wg2/

IPCC, 2014b: Climate Change 2014: Impacts, Adaptation, and Vulnerability. Part B: Regional Aspects. Contribution of Working Group II to the Fifth Assessment Report of the Intergovernmental Panel on Climate Change [Barros, V.R., C.B. Field, D.J. Dokken, M.D. Mastrandrea, K.J. Mach, T.E. Bilir, M. Chatterjee, K.L. Ebi, Y.O. Estrada, R.C. Genova, B. Girma, E.S. Kissel, A.N. Levy, S. MacCracken, P.R. Mastrandrea, and L.L.White (eds.)]. Cambridge University Press, Cambridge, United Kingdom and New York, NY, USA, pp. 688. Available at: http://www.ipcc.ch/report/ar5/wg2/

Local Government Association of South Australia (2012) Guidelines for Developing a Climate Change Adaptation Plan and Undertaking an Integrated Climate Change Vulnerability Assessment. November 2012. http://www.lga.sa.gov.au/webdata/resources/files/Guidelines_for_Developing_a_Climate_Change_Adaptation_Plan.pdf

Maliva R., Missimer Th. (2012) Aridity and Drought, in: Arid Lands Evaluation and Management, Springer, p.21-39.

McMahon TA. Peel MC. Lowe L. Srikanthan R. McVicar TR (2013) Estimating actual. potential. reference crop and pan evaporation using standard meteorological data: a pragmatic synthesis. Hydrol Earth Syst Sci 17: 1331–1363. doi: 10.5194/hess-17-1331-2013.

Oudin L. Andréassian V. Lerat J. Michel C. (2008) Has land cover a significant impact on mean annual streamflow? An international assessment using 1508 catchments. Journal of Hydrology. 357. 303– 316.

Vicente-Serrano SM. Beguería S. Lopez-Moreno JI (2010) A Multi-scalar drought index sensitive global warming: The Standardized Precipitation Evapotranspiration Index – SPEI. Journal of Climate 23: 1696.

Roderick ML. Farquhar GD (2011) A simple framework for relating variations in runoff to variations in climatic conditions and catchment properties. Water Resour. Res.. 47. W00G07. doi:10.1029/2010WR009826.

Spiridonov V. Somot S. Déqué M (2005) ALADIN-Climate: from the origins to present date. ALADIN Newsletter n. 29 (nov. 2005).

Sullivan CA (2011) Quantifying Water Vulnerability: A Multi-Dimensional Approach. Stoch. Env. Res. Risk Assess. p.627–640. 25. 2011.

Thornthwaite CW (1948) An approach toward a Rational Classification of Climate. Geographical Review 38(1): 55-94. Thornthwaite. C. W.. Mather. J. R.. 1957. Instructions and tables for computing potential evapotranspiration and the water balance. Publ. Climatol. 10 (3). 311.

Thornthwaite CW. Mather JR (1957) Instructions and tables for computing potential evapotranspiration and the water balance. Publ. Climatol. 10 (3). 311.

UNEP (1997). World atlas of desertification 2ED. UNEP (United Nations Environment Programme). London. http://www.fao.org/geonetwork/srv/en/metadata.show?id=37040

DRINK ADRIA

UNEP (2009) METHODOLOGIES GUIDELINES; Vulnerability Assessment of Freshwater Resources to Environmental Change. United Nations Environment Programme. Nairobi.

UNEP (2012) Vulnerability Assessment of Freshwater Resources to Climate Change: Implications for Shared Water Resources in the West Asia Region. United Nations Environment Programme. Nairobi.

Vicente-Serrano SM. Beguería S. Lopez-Moreno JI (2010) A Multi-scalar drought index sensitive global warming: The Standardized Precipitation Evapotranspiration Index – SPEI. Journal of Climate 23: 1696.

Vörösmarty CJ. Green P. Salisbury J. Lammers RB (2000) Global Water Resources: Vulnerability from Climate Change and Population Growth. Science. vol. 289: 284-288.

Wochna A. Lange K. Urbanski J (2011) The influence of land cover change during sixty years on nonpoint source phosphorus loads to Gulf of Gdansk. GIS Centre. University of Gdansk . Journal of Coastal Research. ISSN 0749-0208. SI 64. Special Issue.

Zhang L. Potte. N. Hickel K. Zhang Y. Shao Q (2008) Water balance modeling over variable time scales based on the Budyko framework – Model development and testing. Journal of Hydrology. 360. 117-131.

Zhang L. Hickel K. Dawes WR. Chiew FHS. Western AW. Briggs PR (2004) A rational function approach for estimating mean annual evapotranspiration. Water Resour. Res.. 40. W02502. doi:10.1029/2003WR002710.

Zhang L. Dawes WR. Walker GR (2001) Response of mean annual evapotranspiration to vegetation changes at catchment scale. Water Resour. Res. 37. 701–708.

ANNEX 1 – Handling with water demand data

Water demand data for different sectors were gathered and unified in one large MS Excel Spreadsheet, from where they were transformed into GIS environment. Data was collected on NUTS3 statistical level from each country, with two exceptions. For Italy, only selected NUTS3 regions were included in the project (not all of the Italy), and these regions were used in the mask. For Serbia, municipalities were used instead of NUTS regions, as this country is not in the statistical EU NUTS region. One must note that the exact borders of Serbia do not match exactly the country borders of other NUTS3 regions, but the gaps on the border are small and were disregarded in the rasterization process.

To assure the best quality of data they were also compared with data adopted by FAO (available at FAO online database), EUROSTAT database and with WD data from World Bank database. Water use data for partner countries as annual values of water use are presented in Table 1. Discrepancies among data are not big.

All data was saved into a vector shape-file (SHP format) with a file name *SEE_NUTS3_WD_final_ITA.shp*. Please note that in the GIS model picture (Figure 1), the file name is shortened to *NUTS3_SEE* for the increased readability.
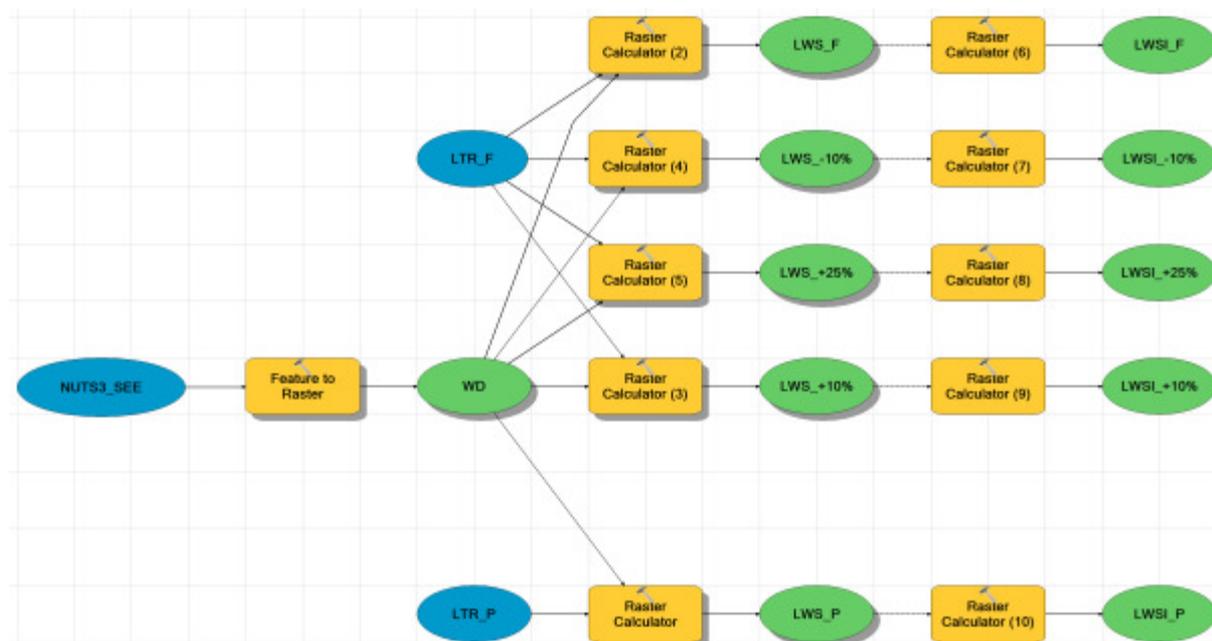
Figure 1: A GIS model of creating maps.

Shape-file contains following attributes: FID and Shape, STAT_LEV for NUTS level, NUTS_ID and NUTS3 for NUTS3 identification, AGRWD for agricultural water demand, DWD for domestic water

demand, INDWD for industrial water demand, WD_tot for total water demand (WD_tot = AGRWD + DWD + INDWD) and DWD_summer (α_{sD}) as a correction factor.

This shape-file was then transformed into several water demand raster layers by ArcGIS (*Feature to raster* tool). Total water demand was rasterized into **WD_tot** layer, agricultural water demand into **AGRWD**, domestic water demand into **DWD**, and industrial water demand into **INDWD** layer.

WD maps were produced on NUTS 3 level in vector format, except for Serbia, for which data was collected on Municipality level. When all WD maps were transformed from vector to raster, "Feature to Raster (Conversion)" was applied. This tool always uses the cell center to decide the value of raster pixel. Thus at the country borders empty cells can be observed.

Regional WR vulnerability - Ljubljana, November 2016

Let's grow up together

DRINK ADRIA

Adriatic IPA
Cross Border Cooperation 2007-2013

DRINK ADRIA